Informes Técnicos Ciemat
1053
Febrero, 2005

MX-80 Bentonite. Thermo-Hydro-Mechanical Characterisation Performed at CIEMAT in the Context of the Prototype Project

M.V. Villar

Departamento de Impacto Ambiental de la Energía

Bentonita MX-80. Caracterización Termo-Hidro-Mecánica Realizada en CIEMAT en el Contexto del Proyecto Prototype

Villar, M.v.

45 pp. 29 figs. 13 refs.

Resumen:

Este documento detalla los resultados de la caracterización termo-hidro-mecánica (THM) de la bentonita MX-80 realizada en CIEMAT entre los años 2001 y 2004 en el contexto del proyecto Prototype, que se lleva a cabo en el laboratorio subterráneo de Äspö (HRL, Suecia). Se ha determinado la presión de hinchamiento y la permeabilidad de la bentonita compactada a diferentes densidades, asi como la influencia de la salinidad del permanente en la conductividad hidraúlica. Se ha estudiado la influencia de la salinidad en la capacidad de retención de la bentonita compactada, para lo que se ha diseñado y puesto a punto una nueva metodología. Se han determinado curvas de retención a volumen constante y a temperaturas de 20 y 60ºC. Se han realizado ensayos edométricos con succión controlada a 20ºC. Finalmente, se ha comparado el comportamiento de la bentonita MX-80 con el de la bentonita española FEBEX.

MX-80 Bentonite. Thermo-Hydro-Mechanical Characterisation Performed at CIEMAT in the Context of the Prototype Project

Villar, M.V.

45 pp. 29 figs. 13 refs.

Abstract:

This document details the results of the thermo-hydro-mechanical (THM) characterisation of the commercial MX-80 bentonite performed by CIEMAT from 2001 to 2004 in the context of a project carried out at the AEspoe Hard Rock Laboratory (Sweden), the Prototype Repository. The swelling pressure and the permeabiliy of the bentonite compacted to different dry densities has been determined, as well as the influence of the permeant salinity on hydraulic conductivity. The influence of salinity on the retention capacity of the compacted bentonite has been studied. For that, a new methodology has been designed. Water retention curves have been determined at temperatures of 20 and 60ºC. Suction controlled oedometer tests have been performed at 20ºC. Finally, the behaviour of the MX-80 bentonite has been compared to that of the Spanish FEBEX bentonite.

CLASIFICACIÓN DOE Y DESCRIPTORES

S12
BENTONITE; RADIONUCLIDE MIGRATION; HYDRAULICS; THERMODYNAMICS PROPERTIES; MECHANICAL PROPERTIES; SALINITY; HYDRAULICS; TEMPERATURE DEPENDENCE

MINISTERIO DE EDUCACIÓN Y CIENCIA

Ciemat
Centro de Investigaciones Energéticas, Medioambientales y Tecnológicas

CIEMAT/DIAE/54540/2/04

MX-80 BENTONITE

THERMO-HYDRO-MECHANICAL CHARACTERISATION PERFORMED AT CIEMAT IN THE CONTEXT OF THE PROTOTYPE PROJECT

M.V. Villar

December 2004

BENTONITA MX-80. CARACTERIZACIÓN TERMO-HIDRO-MECÁNICA REALIZADA EN CIEMAT EN EL CONTEXTO DEL PROYECTO PROTOTYPE

M.V. Villar

39 pp. 29 fig. 13 refs.

Resumen:

Este documento detalla los resultados de la caracterización termo-hidro-mecánica (THM) de la bentonita MX-80 realizada en CIEMAT entre los años 2001 y 2004 en el contexto del proyecto Prototype, que se lleva a cabo en el laboratorio subterráneo de Äspö (HRL, Suecia). Se ha determinado la presión de hinchamiento y la permeabilidad de la bentonita compactada a diferentes densidades, así como la influencia de la salinidad del permeante en la conductividad hidráulica. Se ha estudiado la influencia de la salinidad en la capacidad de retención de la bentonita compactada, para lo que se ha diseñado y puesto a punto una nueva metodología. Se han determinado curvas de retención a volumen constante y a temperaturas de 20 y 60°C. Se han realizado ensayos edométricos con succión controlada a 20°C. Finalmente, se ha comparado el comportamiento de la bentonita MX-80 con el de la bentonita española FEBEX.

MX-80 BENTONITE. THERMO-HYDRO-MECHANICAL CHARACTERISATION PERFORMED AT CIEMAT IN THE CONTEXT OF THE PROTOTYPE PROJECT

M.V. Villar

39 pp. 29 fig. 13 refs.

Abstract:

This document details the results of the thermo-hydro-mechanical (THM) characterisation of the commercial MX-80 bentonite performed by CIEMAT from 2001 to 2004 in the context of a project carried out at the AEspoe Hard Rock Laboratory (Sweden), the Prototype Repository. The swelling pressure and the permeability of the bentonite compacted to different dry densities has been determined, as well as the influence of the permeant salinity on hydraulic conductivity. The influence of salinity on the retention capacity of the compacted bentonite has been studied. For that, a new methodology has been designed. Water retention curves have been determined at temperatures of 20 and 60°C. Suction controlled oedometer tests have been performed at 20°C. Finally, the behaviour of the MX-80 bentonite has been compared to that of the Spanish FEBEX bentonite.

MX-80 BENTONITE.

THERMO-HYDRO-MECHANICAL CHARACTERISATION PERFORMED AT CIEMAT IN THE CONTEXT OF THE PROTOTYPE PROJECT.

Table of contents

1. INTRODUCTION

This report details the results of the thermo-hydro-mechanical (THM) characterisation of the MX-80 bentonite carried out by CIEMAT (Soil Mechanics Laboratory) from 2001 to 2004 in the context of the Prototype Repository project. The participation of CIEMAT in the project – which takes place under contract with ENRESA– has consisted on the performance of laboratory tests to support the HM, THM and THMC modelling work carried out by CIMNE.

The Prototype Repository project is a full-scale test of the KBS-3 concept for high-level radioactive waste disposal that is being conducted at the AEspoe Hard Rock Laboratory (AEHRL, Sweden). It is an integrated test focusing on the engineered barrier system (EBS) performance but comprising also canister deposition, backfilling and plug construction. It is an international, EC-supported activity with the objective to investigate, on a full scale, the integrated performance of EBS and near-field rock of a simulated KBS-3 deep repository in crystalline rock with respect to heat evolution, mechanics, water permeation, ion diffusion, gas migration and microbial processes under natural chemical conditions. The cooperative work aims at accomplishing confidence building as to the capability of constructing safe repositories and predicting EBS performance also for somewhat different conditions than those in the AEHRL.

The Prototype Repository started on September 2000 with the duration time of 42 months. Electrical heaters simulating the waste containers were placed in six vertical holes. The MX-80 bentonite is being used as sealing material around the heaters, either in the form of compacted blocks or of pellets. The blocks have been compacted at dry densities of 1.69 and 1.79 g/cm^3, previously adding water to the bentonite so that to obtain a water content of 17 percent. In this way the initial degree of saturation of the barrier is very high. To fill the gap between the bentonite barrier and the host rock, high-density bentonite pellets have been poured out. On the other hand, the groundwater at the AEHRL is rather salty, and this fact has been taken into account in the design of the tests presented below.

CIMNE, as a subcontractor to ENRESA is performing part of the THM and THMC modelling of the clay barrier behaviour. To support this modelling work, and specifically to improve the knowledge of the hydro-mechanical behaviour of the clay, CIEMAT –under direct contract with ENRESA– has carried out the following laboratory work, which was suggested by the modelling team:

- Hydraulic conductivity tests on the clay compacted to different dry densities and permeated with water of different salinity.
- Determination of retention curves at constant volume for different dry densities and salinities at 20°C.
- Determination of the retention curve at constant volume of the clay compacted at different dry densities and at 60°C.
- Suction controlled oedometer tests, with suctions up to 50 MPa and vertical loads of up to 9 MPa. The initial dry density and water content of the clay in these tests has been that of the blocks manufactured for the *in situ* test.

Besides, the results of swelling pressure tests performed previously at CIEMAT and never reported are also included in this document.

2. MATERIAL

The MX-80 clay is extracted from Wyoming (USA), and has been selected in many disposal concepts as backfilling and sealing material (Sweden, Finland, Germany, France). It is a worldwide known material supplied in the form of powder homoionised to sodium (SKB reports, Müller-Vonmoss & Kahr 1983). The MX-80 bentonite is composed mainly by montmorillonite (65-82%) and it also contains quartz (4-12%), feldspars (5-8%), and smaller quantities of cristobalite, calcite and pyrite. The less than 2 µm fraction of this bentonite is 80-90% of the total. The CEC is 74 meq/100g, and the major exchangeable cations are: Na (61 meq/100g), Ca (10 meq/100g) and Mg (3 meq/100g). The liquid limit of the bentonite is 350-570%, the plastic limit 70% and the specific weight of the solid particles –determined with pycnometers using deionised water as suspension medium– is 2.82.

The MX-80 clay used in the tests performed by CIEMAT was provided in April 1996 by Clay Technology AB (75 kg). Its hygroscopic water content under the CIEMAT laboratories conditions is around 9 percent.

For hydration of the samples either deionised water or saline water are being used. The saline water is obtained in the laboratory by mixing $CaCl_2$ and NaCl at a 32/68 percent ratio to give rise to a solution of 0.5 percent salinity.

3. RESULTS

3.1 Swelling pressure

3.1.1 Methodology

The swelling pressure test makes it possible to determine the equilibrium swelling pressure exercised by a sample on complete saturation at constant volume. For performance of this test, oedometer frames and conventional oedometric cells were used, in which the surface of the oedometer ring was reduced in order to counteract the high pressures expected. Figure 1 shows a schematic cross section of an oedometric cell. The sample is confined in a ring preventing it from deforming laterally, and between two porous stones at its upper and lower surfaces. The piston of the cell, which is adjoined to the upper porous stone, is in contact with the loading ram, whose displacement –or that of the piston itself– may be accurately measured by means of a dial gauge. The sample may be loaded via the ram by means of the system of levers of the oedometric frame on which the cell is located. These cells do not allow the pressure exercised by the sample to be measured directly, but rather determined indirectly from the load that has to be applied in order for the volume of the sample to be kept constant during saturation.

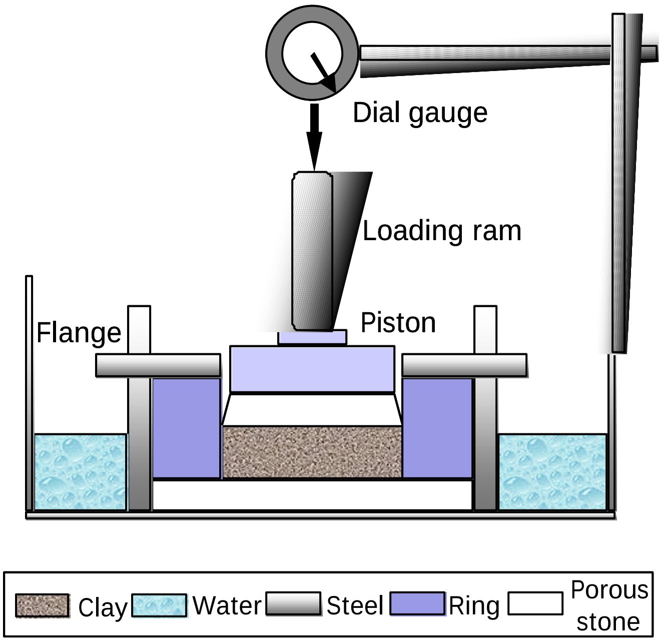

Figure 1: Schematic cross section of an oedometric cell

The samples were prepared by means of uniaxial compaction of the bentonite powder with its hygroscopic water content directly in the oedometer rings. The sample contained in the oedometer ring is placed inside the oedometer cell, which is mounted in the oedometer frame. The lower porous stone is covered with deionised water, such that the sample begins to saturate from the bottom upwards, allowing the air in the pores to escape from the upper part. The displacement recorded by the dial gauge as the sample saturates is observed, and swelling of the sample is prevented by the application of loads. The test is considered to be completed when no strain is observed for at least 24 hours.

The tests were performed at laboratory temperature, which ranged from 20 to 25 °C.

3.1.2 Results

Table I includes the swelling pressure obtained in each test and the initial and final values of dry density and water content, as well as the final degree of saturation of the specimens. Occasionally, and especially for dry densities in excess of 1.60 g/cm^3, the loading capacity of the equipment does not make it possible to completely counteract the deformation of the specimen, as a result of which the final swelling pressure value obtained does not correspond to nominal (initial) dry density but to final dry density, which is lower. It may be appreciated that the degrees of saturation obtained exceed 100 percent, especially for higher dry densities. This is because they were computed considering the density of the water as 1.00 g/cm^3, which was shown to be untrue for high plasticity materials (Villar 2000, 2002, Marcial 2003, Villar & Lloret 2004).

The swelling pressure values are plotted in Figure 1 as a function of the final dry density. It is possible to obtain an exponential fit between swelling pressure (P_s, MPa) and final dry density (ρ_d, g/cm^3):

$$\ln P_s = 6.11\,\rho_d - 7.79 \qquad [1]$$

Table I: Results of swelling pressure tests performed with compacted MX-80 saturated with deionised water

Initial ρ_d (g/cm^3)	**Initial *w* (%)**	**Initial S_r (%)**	**P_s (MPa)**	**Duration (days)**	**Final *w* (%)**	**Final ρ_d (g/cm^3)**	**Final S_r (%)**
1.08	11.1	19	0.4	43	59.1	1.07	102
1.20	9.1	19	0.5	13	53.1	1.20	110
1.20	8.9	19	0.4	35	50.9	1.20	107
1.28	10.0	24	1.3	89	42.4	1.28	100
1.39	9.3	26	1.8	14	37.6	1.38	102
1.48	10.2	32	4.1	89	32.9	1.48	102
1.49	9.4	30	3.4	14	34.0	1.47	104
1.59	9.6	35	5.3	14	31.7	1.55	109
1.69	9.6	41	11.6	43	28.7	1.68	120

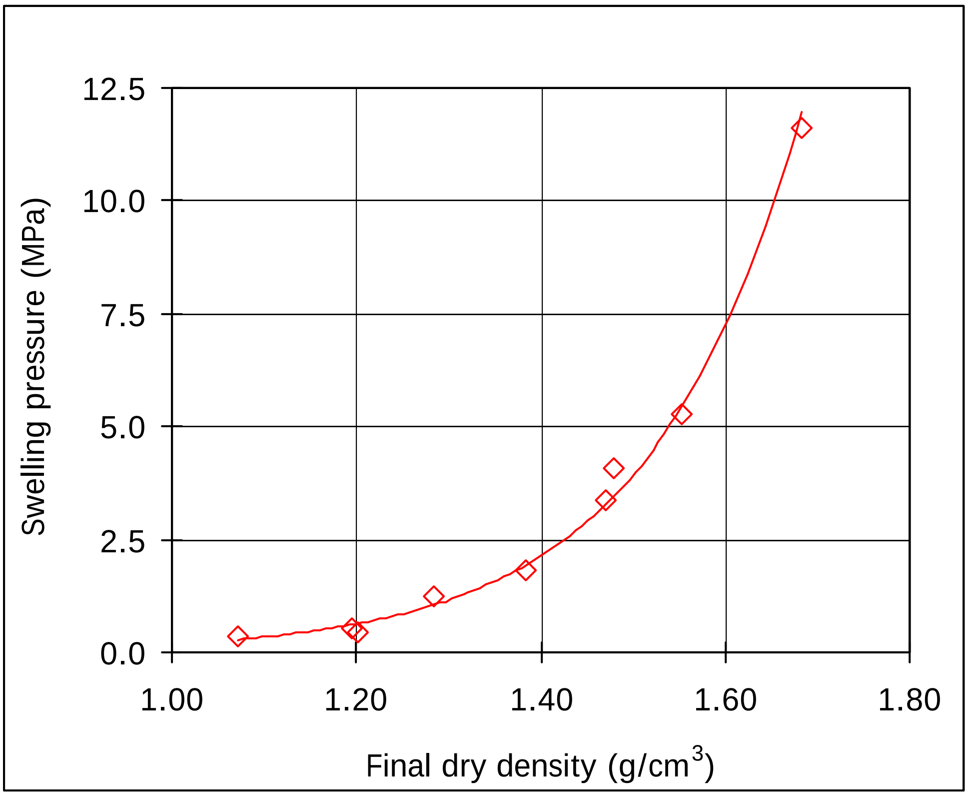

Figure 1: Swelling pressure of compacted MX-80 saturated with deionised water

3.2 Hydraulic conductivity

3.2.1 Methodology

A method for the measurement of hydraulic conductivity in expansive soils through the determination of the coefficient of permeability has been developed at CIEMAT. The theoretical principle on which the method is based is that of the fixed load permeameter. Basically, it consists on measuring against time the volume of water that passes through a specimen, confined in a rigid cell preventing it from deforming, to which is applied a constant hydraulic gradient between the upper and lower parts. For this purpose a hydraulic head, that is to say, a difference in potential, is applied between the upper and lower parts of the previously saturated sample. The complete saturation of the sample and associated swelling guarantee perfect contact with the walls of the cell, preventing the flow of water between these and the sample. At the same time, the flow of water passing through the specimen is measured versus time.

The measuring system is made up of the following elements (Figure 2):

- Stainless steel cell consisting on a cylindrical ring in which the sample is confined and two covers on top and bottom with water inlet/outlets. The dimensions of the sample are 19.63 cm^2 in surface area and 2.50 cm in length.

- Two pressure systems, for injection and downstream pressures. The system used for downstream pressure consists of a set of self-compensating mercury deposits equipped with an installation for deaerated water, while for injection pressure, Wykeham Farrance electrohydraulic constant pressure systems (for pressures of up to 3.5 MPa) or Gilson piston pumps (of the type used for high precision liquid chromatography – HPLC) are used.

- Electronic volume change measurement system, with an accuracy of 0.001 cm^3.

- Data acquisition system.

The clay, with its hygroscopic water content, is directly compacted inside the cell ring. Once the permeability cell mounted, the samples have been saturated at 0.6 MPa from both faces with the same kind of water than that to be used later in the determination of the hydraulic conductivity (deionised or saline). Once the sample is saturated, the hydraulic gradient is applied by increasing the injection pressure at the lower part of the cell, while the downstream pressure is maintained at 0.6 MPa, in order to favour the dissipation of air in the system. The values of hydraulic head applied have ranged from 0.6 MPa to 3.4 MPa, depending on the dry density of the specimen. The automatic volume change apparatus periodically records the volume of water passing through the sample. Once constant flow is achieved, permeability is calculated by applying Darcy’s law.

The final water content and dry density of the specimen is checked on completion of the test, by drying the sample at 110°C during 24 hours.

The determinations have been made at laboratory temperature (between 20 and 25 °C). For the use of saline water as permeant, adequate deposits have been placed at the entrance and exit of the permeability cell.

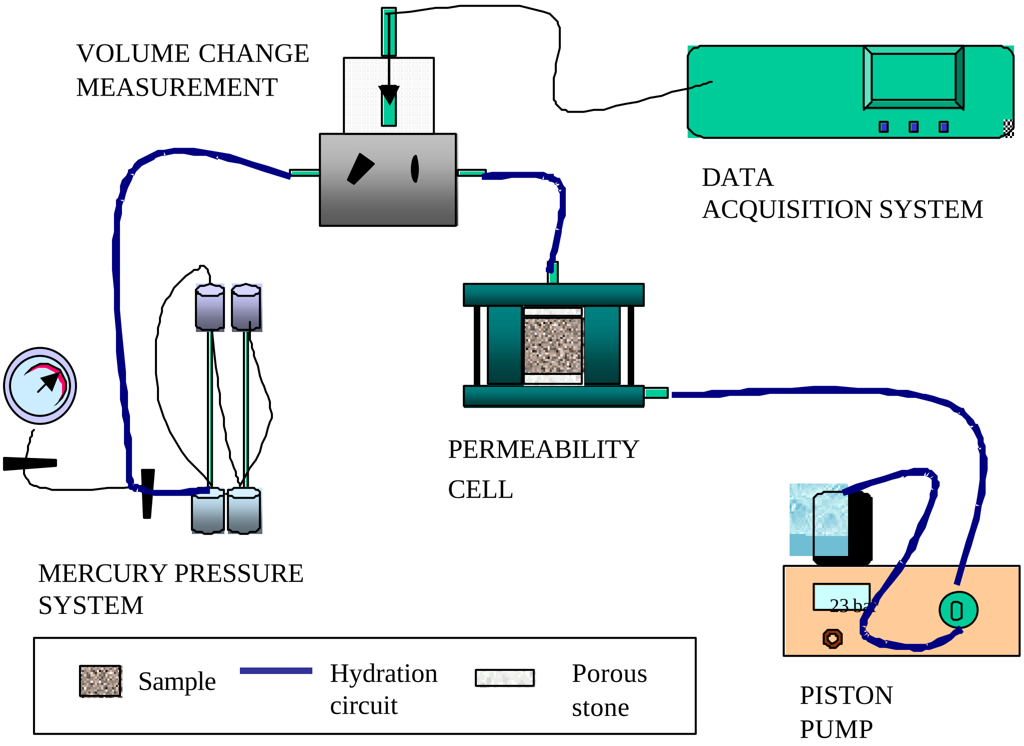

Figure 2: Schematic representation of permeability measuring assembly for expansive soils

3.2.2 Results

The results obtained in the hydraulic conductivity tests performed with bentonite compacted at different dry densities are shown in Table II, for samples saturated and permeated with deionised water, and in Table III, for samples saturated and permeated with saline water.

Table II: Results of the hydraulic conductivity tests using deionised water as permeant

r $_d$ (g/cm^3)	**Initial *w* (%)**	**Initial S_r (%)**	***k* (m/s)**	**Final *w* (%)**	**Final S_r (%)**
1.39	10.1	26	$1.2 \cdot 10^{-12}$	37.7	103
1.39	8.9	24	$3.8 \cdot 10^{-13}$	36.8	101
1.49	9.6	28	$3.0 \cdot 10^{-13}$	32.8	104
1.49	9.0	28	$4.2 \cdot 10^{-13}$	33.0	104
1.58	9.5	34	$1.8 \cdot 10^{-13}$	29.5	106
1.59	9.7	33	$2.0 \cdot 10^{-13}$	28.5	104
1.68	9.2	38	$5.1 \cdot 10^{-14}$	24.8	104

Table III: Results of the hydraulic conductivity tests using saline water (0.5 %) as permeant

r $_d$ (g/cm^3)	**Initial *w* (%)**	**Initial S_r (%)**	***k* (m/s)**	**Final *w* (%)**	**Final S_r (%)**
1.29	9.8	23	$2.1 \cdot 10^{-12}$	43.6	104
1.35	9.4	24	$8.6 \cdot 10^{-13}$	46.3	119
1.39	8.6	24	$6.4 \cdot 10^{-13}$	38.9	107
1.45	9.4	28	$5.8 \cdot 10^{-13}$	36.8	109
1.49	8.9	28	$3.1 \cdot 10^{-13}$	32.6	103
1.59	8.8	32	$2.4 \cdot 10^{-13}$	29.3	107
1.64	8.3	33	$3.1 \cdot 10^{-13}$	26.2	103
1.65	8.5	34	$2.2 \cdot 10^{-13}$	26.6	106
1.69	8.8	37	$1.2 \cdot 10^{-13}$	24.8	105

These results are plotted in Figure 2, where exponential relations between dry density (ρ_d, g/cm^3) and hydraulic conductivity (*k*, m/s) have been drawn for each kind of permeant:

For deionised water: $\log k = -2.94\ \rho_d - 8.17$ [2]

For saline water: $\log k = -2.39\ \rho_d - 8.78$ [3]

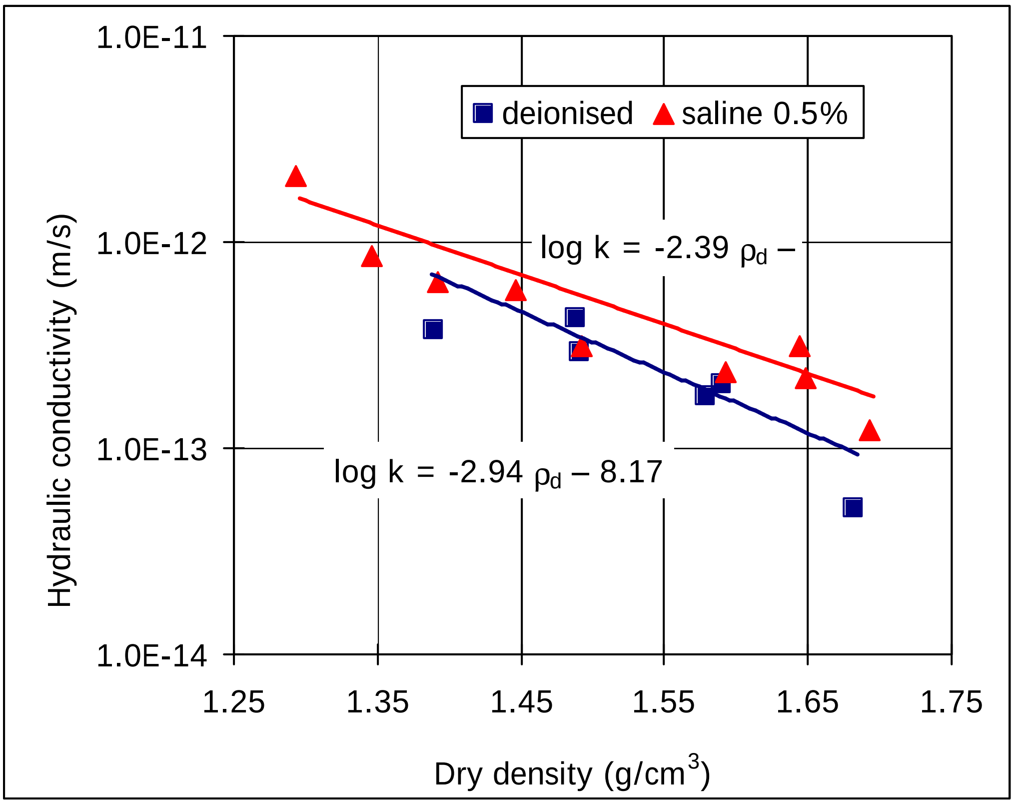

Figure 2: Results of the hydraulic conductivity tests with compacted MX-80 as a function of the kind of permeant

The hydraulic conductivity is on average 135 percent higher when saline water is used as permeant. If this is evaluated taking into account that the values of permeability are of the order 10^{-13} m/s, the difference does not seem to be drastic. Karnland *et al.* 1992 found an increase of the permeability of compacted MX-80 of half an order of magnitude when the salinity of the permeant was increased from 0 to 3.5 NaCl percent.

3.3 Retention curve at laboratory temperature

3.3.1 Methodology

To determine the retention curve at constant volume and as a function of the salinity of the interstitial water, a new method has been designed. It consists on the measurement, through a capacitive sensor, of the relative humidity of blocks of clay compacted to different dry densities and water contents. The bentonite is previously mixed with the desired quantity and kind of water, and this paste is kept for two days in a plastic bag to allow the homogenisation of the moisture. Afterwards, the moistened clay is uniaxially compacted at the desired density in a steel mould of nominal dimensions 10x4x3 cm. The blocks thus obtained are allowed to stabilise for at least two days wrapped in paraffin foil and, afterwards, a hole is drilled in them to allow a relative humidity sensor to be installed inside (Figure 3). The transmitters used are ROTRONIC HYGROMETER® CK90, that include a humidity sensor (I-400) which changes its electrical characteristics with extremely small variations in humidity (capacitive type relative humidity sensor). They include also a temperature sensing system (Pt 100). The accuracy of the humidity sensor at 23°C is ±1.5 percent over the range 0-100 percent RH. The clay block-sensor assembly is kept inside a closed plastic bag during the measurement (Figure 4). The relative humidity and temperature values are checked periodically until stabilisation, which takes place usually very quickly, although, as a rule, the values measured after 24 hours have been taken. To convert the values of relative humidity (*RH*, %) to suction values (*s*, MPa) the Kelvin's law has been used:

$$s = -10^{-6} \frac{R \times T}{V_{\mathrm{w}}} \ln\left(\frac{RH}{100}\right) \qquad [4]$$

where R is the universal constant of gases (8.3143 J/mol·K), T the absolute temperature and V_{w}, the molar volume of water ($1.80 \cdot 10^{-5}$ m^3/mol).

Once the measurement phase accomplished, the sensor is extracted from the block, and the latter is measured, weighed and placed in an oven at 110°C to check its final dry density and water content. Two similar blocks were manufactured and measured at a time.

Figure 3: Bentonite compacted block with a hole drilled for the insertion of the *RH* sensor

Figure 4: Measurement of the relative humidity inside a block of bentonite

3.3.2 Results

Four dry densities, 1.50, 1.60, 1.70 and 1.80 g/cm^3, have been investigated, with water contents of the clay from 8 (the hygroscopic one) to 25 percent. The target water contents were obtained by mixing previously the clay with deionised or saline water (0.5 percent salinity). The results obtained are shown in Table IV and Table V and plotted in Figure 5 and Figure 6. The compaction technique does not allow to manufacture blocks of degree of saturation in excess of 80 percent, for which reason, no results on suction are available for such high humidities. It neither allows compacting blocks with water content below the hygroscopic one, as they lack cohesion and crumble easily. Consequently, no results can be obtained for the lowest degrees of saturation.

Table IV: Results of the tests for determination of the retention curve with deionised water

Reference	***w* (%)**	**ρ_d (g/cm^3)**	**S_r**	***RH* (%)**	***T* (°C)**	**Suction (MPa)**
1.5_8_1	9.2	1.43	0.27	45.4	20.1	107
1.5_8_2	9.3	1.43	0.27	45.8	20.4	106
1.5_10_1	10.3	1.46	0.31	51.9	18.8	88
1.5_10_2	10.2	1.46	0.31	51.9	19.2	88
1.5_15_1	14.9	1.47	0.46	67.6	20.9	53
1.5_15_2	15.0	1.47	0.46	67.1	21.3	54
1.5_17_1	17.0	1.47	0.52	73.9	18.6	41
1.5_17_2	17.0	1.47	0.52	73.1	19.0	42
1.5_20_1	19.8	1.49	0.62	83.5	20.0	24
1.5_20_2	19.8	1.48	0.61	82.6	20.3	26
1.5_23_1	22.8	1.48	0.71	89.3	18.9	15
1.5_23_2	22.9	1.48	0.72	88.4	19.4	17
1.5_25_1	24.6	1.49	0.78	92.1	17.1	11
1.5_25_2	24.7	1.49	0.78	91.0	17.4	13
1.6_8_1	8.5	1.53	0.29	46.5	23.3	105
1.6_8_2	8.5	1.53	0.28	44.8	23.6	110
1.6_10_1	10.4	1.54	0.35	54.3	23.1	83
1.6_10_2	10.4	1.55	0.36	54.4	23.1	83
1.6_15_1	14.8	1.54	0.51	68.6	23.0	51
1.6_15_2	14.8	1.57	0.52	67.9	23.4	53
1.6_17_1	16.4	1.56	0.57	74.1	23.1	41
1.6_17_2	16.3	1.51	0.53	72.8	23.4	43
1.6_20_1	18.3	1.58	0.66	79.3	23.0	32
1.6_20_2	18.1	1.58	0.65	78.7	23.3	33
1.6_23_1	22.0	1.57	0.78	88.0	24.4	18
1.6_23_2	22.0	1.57	0.78	87.3	24.6	19
1.7_8_1	8.7	1.68	0.36	44.1	18.8	110
1.7_8_2	8.7	1.68	0.36	44.8	19.3	108
1.7_8_3	8.6	1.68	0.36	43.3	19.4	113
1.7_10_1	10.5	1.62	0.40	54.0	18.5	83
1.7_10_2	10.6	1.63	0.41	54.0	18.1	83
1.7_15_1	15.5	1.64	0.60	68.5	19.1	51

Reference	***w* (%)**	r $_d$ **(g/cm^3)**	S_r	***RH* (%)**	***T* (ºC)**	**Suction (MPa)**
1.7_15_2	15.1	1.64	0.59	64.5	18.6	59
1.7_17_1	17.4	1.65	0.70	74.9	20.9	39
1.7_17_2	18.3	1.64	0.72	75.2	20.4	39
1.7_20_1	19.1	1.67	0.78	79.8	20.4	31
1.7_20_2	19.5	1.67	0.79	79.8	20.8	31
1.8_8_1	8.2	1.70	0.35	41.1	21.9	121
1.8_8_2	8.2	1.73	0.37	41.1	22.4	121
1.8_10_1	11.0	1.71	0.48	53.6	21.5	85
1.8_10_2	11.0	1.70	0.47	53.6	21.9	85
1.8_15_1	15.8	1.70	0.68	68.5	21.9	51
1.8_15_2	15.8	1.70	0.68	67.8	22.3	53
1.8_17_1	17.5	1.74	0.80	73.1	19.5	42
1.8_17_2	17.3	1.75	0.79	72.6	19.9	43

Table V: Results of the tests for determination of the retention curve with saline water (0.5 percent salinity)

Reference	***w* (%)**	r $_d$ **(g/cm^3)**	S_r	***RH* (%)**	***T* (ºC)**	**Suction (MPa)**
S1.5_10_1	10.3	1.44	0.30	51.8	16.6	88
S1.5_10_2	10.3	1.45	0.32	51.7	16.9	88
S1.6_10_1	10.0	1.54	0.36	54.1	23.0	84
S1.6_10_2	10.1	1.54	0.36	53.9	23.5	85
S1.6_15_1	14.9	1.56	0.55	68.6	24.0	52
S1.6_15_2	14.9	1.55	0.54	68.6	24.4	52
S1.6_17_3*	16.9	1.56	0.62	75.9	22.3	38
S1.6_17_4*	16.8	1.55	0.61	75.1	22.6	39
S1.6_17_1*	18.5	1.55	0.67	80.6	23.0	29
S1.6_17_2*	18.5	1.55	0.67	80.0	23.1	30
S1.6_20_1*	18.7	1.58	0.71	80.2	22.8	30
S1.6_20_2*	18.5	1.58	0.70	79.2	22.9	32
S1.6_23_1*	22.4	1.59	0.87	88.6	22.9	16
S1.6_23_2*	22.4	1.59	0.86	87.5	22.9	18
S1.7_10_1	10.6	1.65	0.45	54.5	21.5	82
S1.7_10_2	10.6	1.65	0.45	54.5	21.5	82

Reference	***w* (%)**	**ρ_d (g/cm^3)**	**S_r**	***RH* (%)**	***T* (ºC)**	**Suction (MPa)**
S1.7_15_1	15.2	1.66	0.65	68.7	23.8	51
S1.7_15_2	14.8	1.51	0.51	67.8	24.3	53
S1.7_17_1	16.7	1.64	0.70	73.3	24.3	43
S1.7_17_2	16.9	1.65	0.71	73.7	24.6	42
S1.7_20_1	19.8	1.66	0.85	81.8	23.4	28
S1.7_20_1	20.0	1.66	0.85	81.8	23.9	28
S1.8_10_1	11.1	1.71	0.52	54.0	21.2	84
S1.8_10_2	11.1	1.71	0.52	53.9	21.7	84
S1.8_15_1	16.1	1.69	0.72	68.8	20.9	51
S1.8_15_2	16.1	1.71	0.75	67.9	21.2	52
S1.8_17_1	17.5	1.75	0.87	72.8	20.5	43
S1.8_17_2	17.7	1.73	0.85	72.2	20.9	44

*tests in which the clay was mixed with water of salinity 1.2 percent

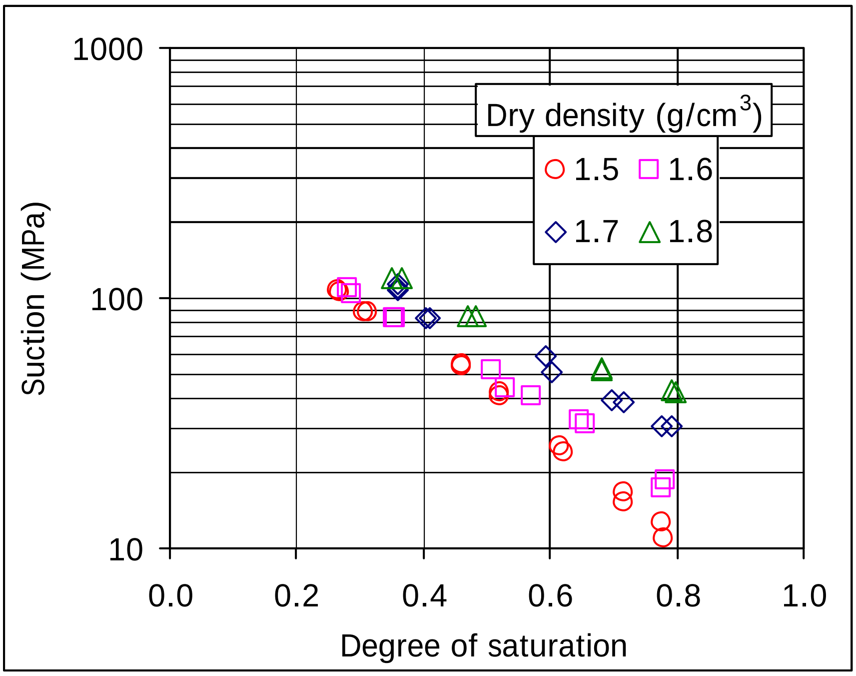

Figure 5: Retention curve for MX-80 clay compacted at different dry densities and water contents (deionised water)

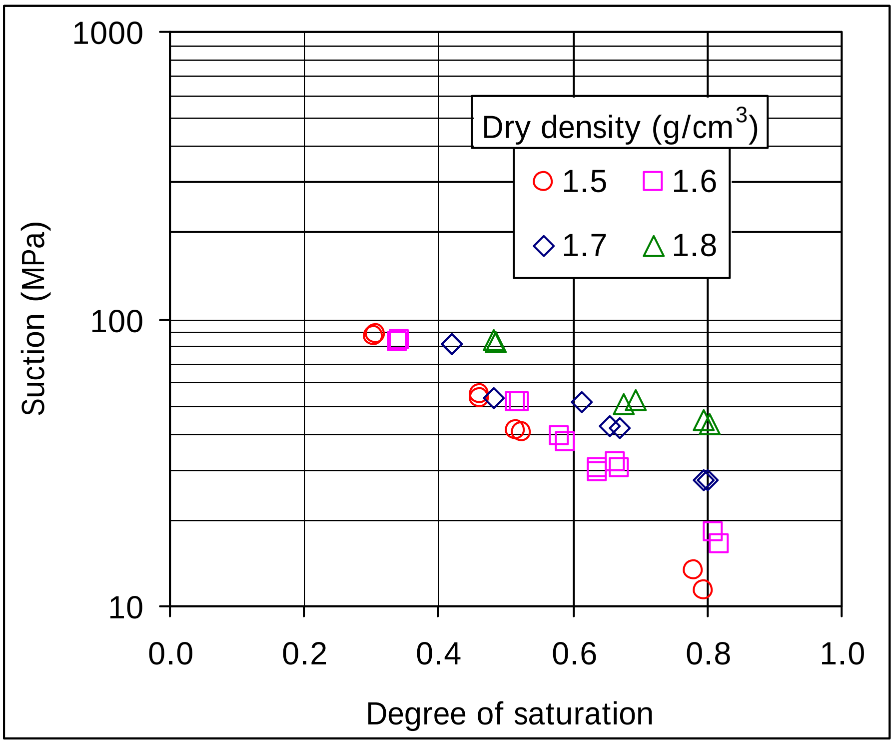

Figure 6: Retention curve for MX-80 clay compacted at different dry densities and water contents (saline water)

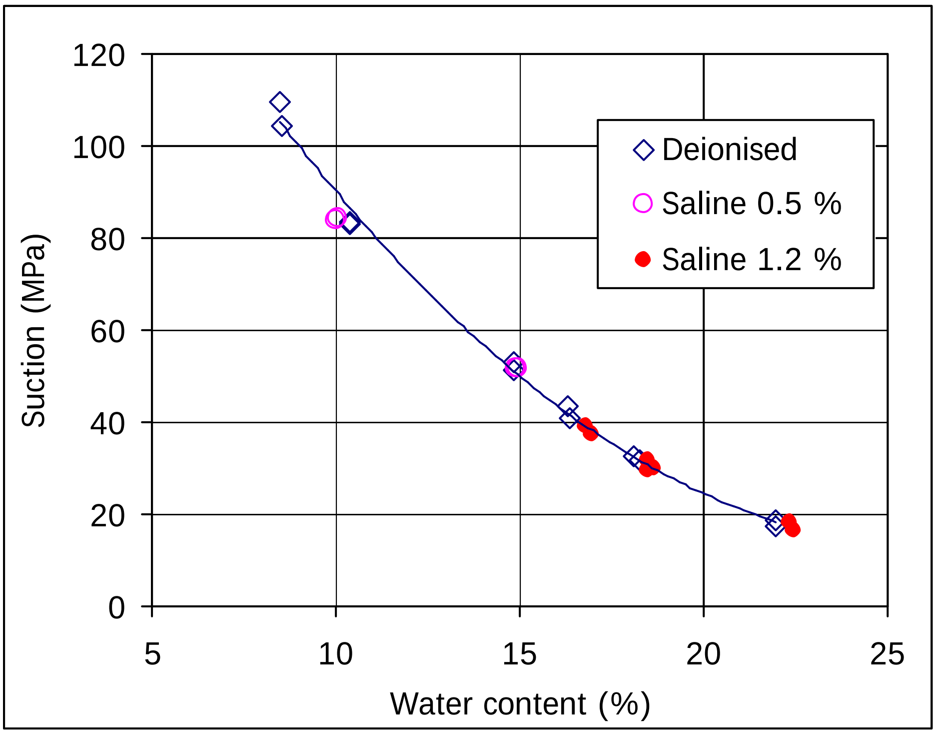

Figure 7: Suction/water content relation for MX-80 clay compacted at dry density 1.60 g/cm^3 with different kinds of water

The results clearly show the dependence of suction on degree of saturation, being the suction of a block of a given degree of saturation higher the higher the dry density of the block.

With the results available it has not been possible to distinguish the influence of the salinity of the interstitial water on the value of suction. In fact, the suctions measured for a given dry density and water content of the clay are the same regardless the salinity of the water added. As an example, the values obtained for the blocks compacted at a nominal dry density of 1.6 g/cm^3 with different kinds of water are shown in Figure 7.

The results obtained have been fitted to the van Genuchten expression (van Genuchten 1980) using the code RETC (van Genuchten *et al.* 1991), with which the parameters θ_s (saturated volumetric water content), θ_r (residual volumetric water content), α and m (empirical constants) are simultaneously derived. The expressions considered are:

$$\theta_e = \left[\frac{1}{1+(\alpha h)^{1/(1-m)}}\right]^m \qquad [5]$$

$$\theta_e = \frac{\theta - \theta_r}{\theta_s - \theta_r} \qquad [6]$$

where θ_e is the effective volumetric water content and h is the soil water pressure head, expressed in m. In this particular form of the expression, m is equal to $1-(1/n)$, where n is another empirical constant. Suction has been expressed as potential (m) and the gravimetric water contents have been converted into volumetric water contents by taking into account the dry density of the specimens. The parameters found through the fitting are shown in Table VI and the experimental points and fittings are plotted in Figure 8 for deionised water and Figure 9 for saline water.

Table VI: Parameters of the van Genuchten expression fitted to the retention curves for MX-80 clay

Dry density (g/cm^3)	**Kind of water**	α	θ_s	***n***
1.50	Deionised	0.0004	0.51	1.79
	Saline	0.0003	0.50	1.97
1.60	Deionised	0.0003	0.47	2.00
	Saline	0.0004	0.51	1.88
1.70	Deionised	0.0002	0.48	2.08
	Saline	0.0002	0.48	2.15
1.80	Deionised	0.0003	0.56	2.04
	Saline	0.0002	0.54	2.20

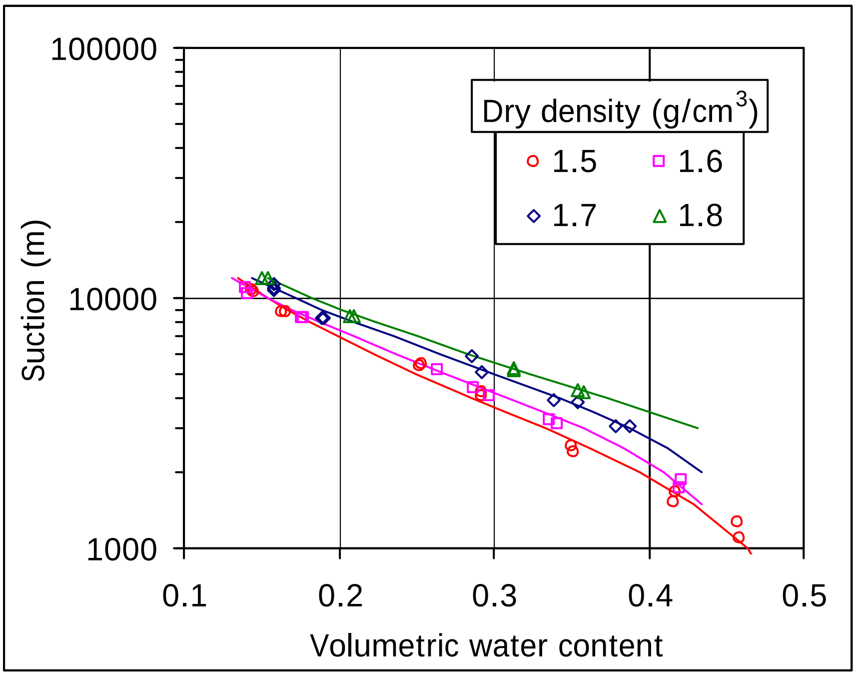

Figure 8: van Genuchten fittings (lines) for the retention curves obtained with deionised water

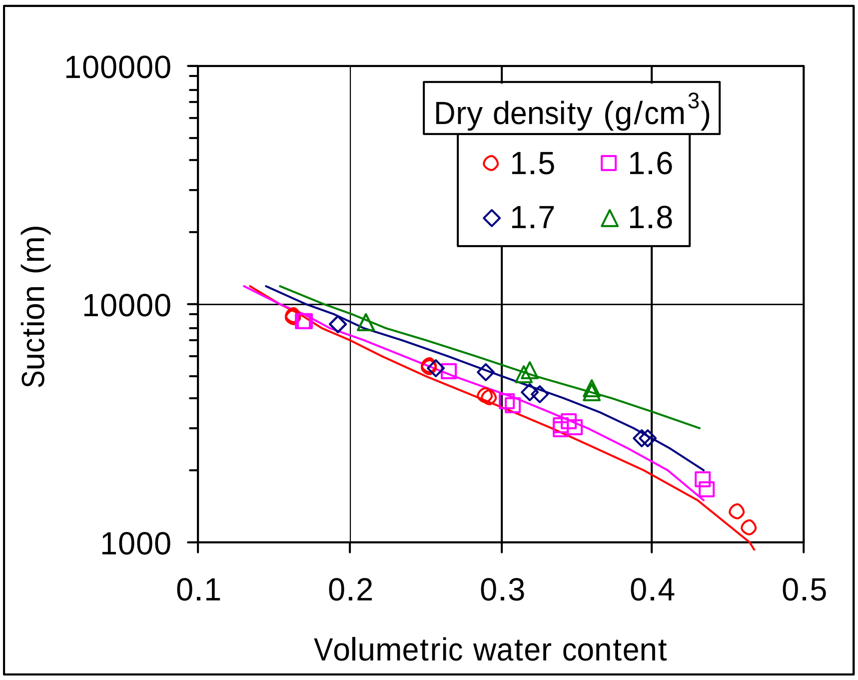

Figure 9: van Genuchten fittings (lines) for the retention curves obtained with saline (0.5 percent) water

In order to check the performance of this new methodology, a retention curve at 20°C has also been determined in non-deformable cells, according to the method described in the following section, which has been thoroughly tested in the context of FEBEX and FEBEX II Projects. With this aim, a wetting/drying path for dry density 1.60 g/cm^3, from an initial water content of 9 percent (the hygroscopic one, approximate suction 110 MPa) has been performed in a non-deformable cell. The results obtained are shown in Table VII and plotted in Figure 10, along with the results obtained with the sensor/block method for the same dry density (results for deionised water, Table IV). It can be checked the good correlation between both methods. The advantage of the method of the block and the sensor, designed for the Prototype Project, is that it is much easy and quick to get results with it. It has the drawback that, in its present configuration, it is neither applicable to suctions below 20 MPa nor at high temperatures.

Table VII: Results of the wetting path performed with MX-80 compacted at ρ_d 1.60 g/cm^3 with initial water content 9 percent

Suction (MPa)	***w* (%)**	**S_r (%)**
124.1	8.2	30
71.2	11.0	41
33.0	16.5	61
19.9	19.3	71
10.9	21.6	80
4.3	24.6	91
1.3	26.6	98

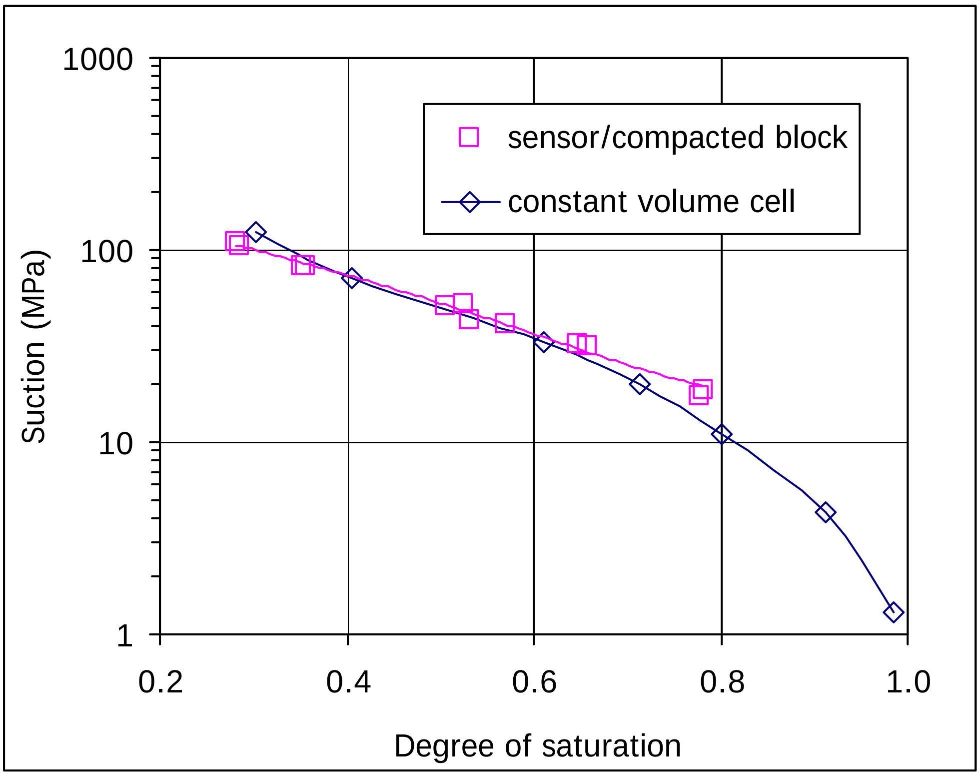

Figure 10: Retention curves at 20°C determined with two different methods for MX-80 clay compacted at dry density 1.60 g/cm^3

3.4 Retention curve at 60°C

3.4.1 Methodology

The retention curves at 60°C are being determined in non-deformable cylindrical cells designed to prevent variations in the volume of the sample. These cells consist of a cylindrical body measuring 0.5 cm in thickness, with two perforated covers joined by bolts. All the elements were manufactured from high corrosion-resistant stainless steel (Figure 11).

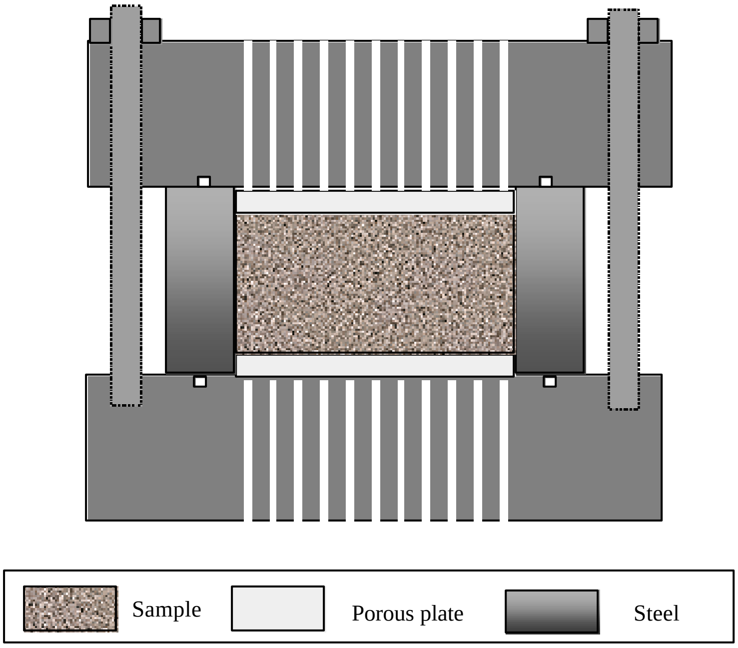

Figure 11: Non-deformable cell for the determination of the retention curve

The sample is compacted directly inside the cell, from the powder clay at the desired water content. The length of the specimens is 1.20 cm and their cross section 3.80 cm^2. A porous stone and Whatmann 54 filter paper are placed between the covers of the cell and the sample. The cell is placed in a desiccator with a sulphuric acid solution and vacuum is created. The suction control method is, therefore, through the control of relative humidity.

The porous stone and the perforated covers allow for the exchange of water in the vapour phase between the clay and the atmosphere of the desiccator. This process is very slow, not only because not the entire surface of the sample acts as an exchange surface (but just the upper and lower parts) but also because the process is performed at constant volume. Periodically (every 3 or 4 weeks, in view of the slowness of the process), a check is made of the variation in weight of the sample, and thus of its water content. Once equilibrium is reached, the solution in the desiccator is changed and its density checked, in order to calculate the suction applied at each step.

For determination of the retention curves at 60°C, the desiccator is placed inside an oven with regulated temperature, where it remains until weighing of the samples and changing of the solution (Figure 12). Measurement of the density of the solution removed from the desiccator is performed with pycnometers at 20°C, that is to say, following cooling. There is an experimental relation between the specific gravity (or density) of the solution (d, g/cm^3) and the percentage in weight of the sulphuric acid in the solution (p), which is temperature-dependent (Lide 1995). For 20°C, this relation may be adjusted to an exponential equation:

$$p = 145.8984 \times \ln(d) + 0.9807 \qquad [7]$$

The relation between the weight percentage of the solution and its activity (a_w) is established taking into account the temperature at which the determination was performed. For 60°C this ratio is as follows (Gmitro & Vermeulen 1964):

$$a_w = 8 \cdot 10^{-8} p^4 - 8 \cdot 10^{-6} p^3 - 7 \cdot 10^{-5} p^2 - 0.0048p + 1.0018 \qquad [8]$$

Likewise, the calculation of suction on the basis of relative humidity ($RH = a_w/100$) is accomplished by including the adequate temperature in the Kelvin's equation (Equation 4).

The cells only prevent variations in the volume of the sample when swelling occurs, that is to say, in the event of wetting, but not when there is shrinkage.

Figure 12: Desiccators with non-deformable cells inside the oven at the moment of vacuum generation

3.4.2 Results

To determine the retention curves at 60°C, the paths followed have been chosen taking into account the possible evolution of the clay in the barrier.

- Wetting paths for dry density 1.79 and 1.60 g/cm^3, from an initial water content of 16 percent (approximate suction 50 MPa). This would be the situation of the blocks in the outer part of the barrier.

- Drying/wetting paths for dry densities 1.79 and 1.37 g/cm^3 (the latter value should have been 1.60 g/cm^3, but there was a mistake in the preparation of the specimens), from an initial water content of 16 percent (approximate suction 50 MPa). This would be the situation of the blocks in the inner part of the barrier.

- Wetting paths for dry density 1.30 g/cm^3, from an initial water content of 9 percent (the hygroscopic one, approximate suction 110 MPa). These are the conditions of the pellets that fill the gap between the barrier and the host rock.

The results obtained are shown in Table VIII to Table X and plotted in Figure 13. It can be observed that the degrees of saturation are higher than 1, as they have been computed considering the density of the adsorbed water equal to 1.00 g/cm^3, as for free water. The retention curves barely show hysteresis, and the behaviour in the wetting, wetting after drying and drying paths is rather similar.

Table VIII: Results of the wetting paths performed at 60°C with MX-80 compacted at different dry densities with initial water content 16 percent

r$_d$ (g/cm^3)	**1.37**		**1.79**	
Suction (MPa)	***w* (%)**	**S_r (%)**	***w* (%)**	**S_r (%)**
52	14.4	39	14.1	69
30	17.6	47	16.8	82
15	20.3	55	18.9	93
7	24.9	67	21.2	104
1	30.1	81	23.6	116

Table IX: Results of the drying/wetting paths performed at 60°C with MX-80 compacted at different dry densities with initial water content 16 percent

r$_d$ (g/cm^3)	**1.60**		**1.79**	
Suction (MPa)	***w* (%)**	**S_r (%)**	***w* (%)**	**S_r (%)**
51	14.9	55	14.8	72
76	12.3	45	12.5	61
121	8.7	32	8.8	43
105	9.2	34	9.3	45
61	13.4	50	13.1	64
41	16.0	59	15.6	76
29	16.9	62	16.4	80

r d (g/cm^3)	**1.60**		**1.79**	
Suction (MPa)	***w* (%)**	**S_r (%)**	***w* (%)**	**S_r (%)**
6	23.8	88	21.2	104

Table X: Results of the wetting path performed at 60°C with MX-80 compacted at ρ_d 1.30 g/cm^3 with initial water content 9 percent

Suction (MPa)	***w* (%)**	**S_r (%)**
125	7.6	18
70	11.5	28
51	13.9	34
36	16.8	40
17	20.0	48
18	20.5	49
0.3	36.7	88

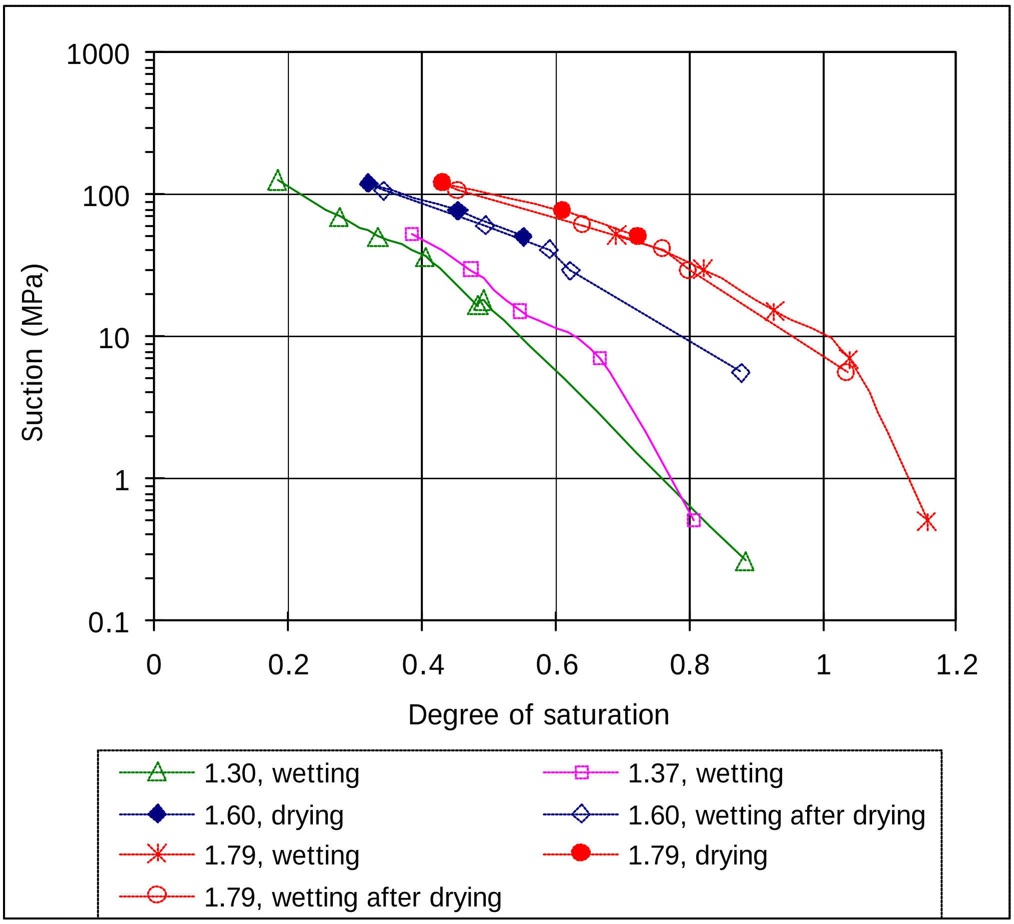

Figure 13: Retention curves at constant volume and at 60°C for MX-80 clay (dry densities in g/cm^3)

Figure 14 presents the comparison of some of the curves obtained at 60°C with the cells method and some curves obtained at 20°C with the sensor/block method (see previous section). For a given dry density, the retention capacity seems to be slightly higher at high temperature, at least for suctions above 30 MPa. However, this must not be considered as a definitive conclusion, since the density of the blocks used to determine the curves with the sensor/block method is usually lower than the nominal value (see Table IV), and it has been seen that density has a decisive influence on the retention capacity. In fact, if the curves obtained with the cell method at 20°C (Table VII) and 60°C (Table IX) for the bentonite compacted at 1.60 g/cm^3 are compared (Figure 15), no differences can be noticed. Therefore, it can be concluded that the effect of temperature on the retention capacity must be very small at least for temperatures of up to 60°C.

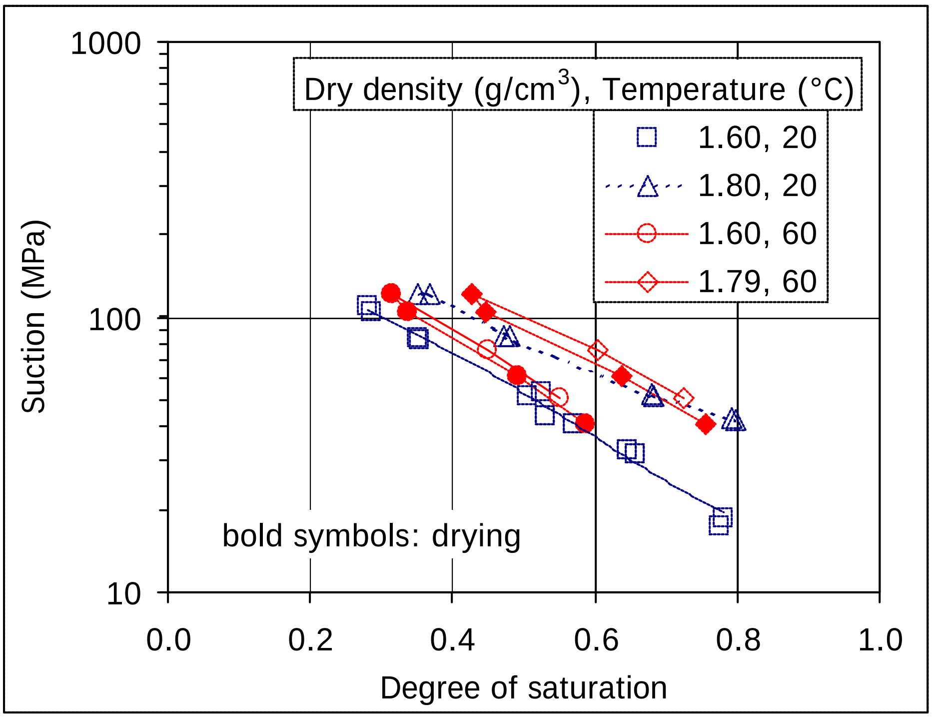

Figure 14: Retention curves for MX-80 at 20°C (sensor and block method) and 60°C (cells method)

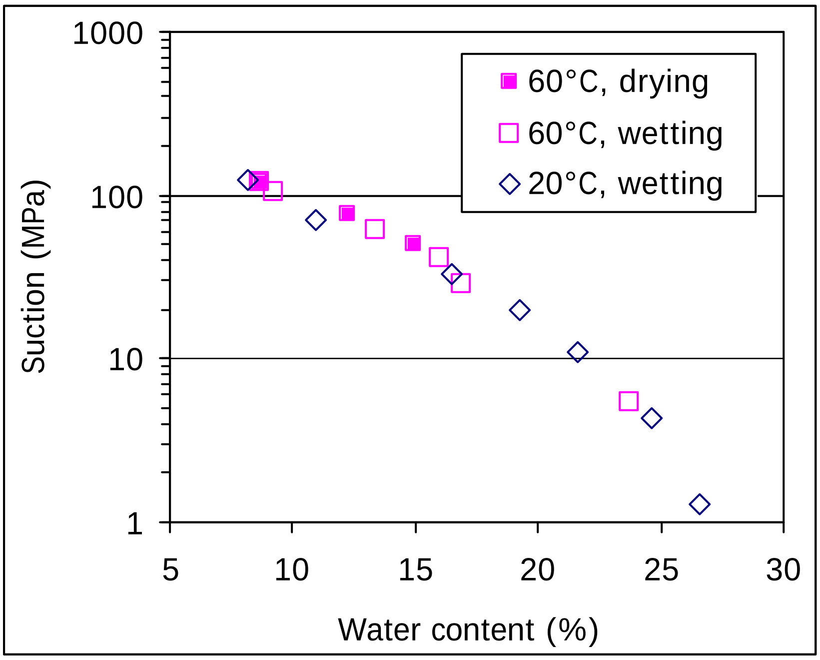

Figure 15: Retention curves obtained with the cells method for MX-80 at 20°C and 60°C

3.5 Suction controlled oedometer tests

The oedometric test makes it possible to study the one-dimensional compressibility of soils. Thanks to this, it is possible to determine the speed and magnitude of the consolidation of a laterally confined soil when axially loaded and drained. When oedometric tests are performed with controlled suction, an additional state variable is introduced in the system of stresses, suction. This means that the sample, in addition to undergoing modifications in vertical stress, is subjected to different suctions during the test. Thus, the suction may be kept constant throughout the loading process, or drying or wetting paths may be experimented, by increasing or decreasing suction, while the vertical stress remains constant.

3.5.1 Methodology

Two techniques have been used to control suction: axis translation and the imposition of relative humidity. In both cases, suction is applied but is not measured. The axis translation technique allows the control only of matric suction, while the control of the relative humidity modifies the total suction. The axis translation is achieved by injecting nitrogen in a membrane cell, and the control of the relative humidity by using sulphuric acid solutions. Specifically, suction has been applied by nitrogen pressure for values between 0.1 and 14 MPa, and by solutions of sulphuric acid for values between 1 and 50 MPa.

The membrane cell for application of nitrogen pressure is manufactured in stainless steel and consists of a base, cover and central body (Figure 16). The cover of the cell has a gas inlet with a manometer for values of up to 16 MPa. The base of the cell has an embedded porous stone, below which there are two inlet and outlet orifices, connected to a burette with water at atmospheric pressure. A semipermeable, regenerated cellulose membrane is placed over this stone, with the sample resting directly on it. This membrane allows water and ions to pass, but not gas. A peristaltic pump, installed between the burette and the cell inlets, facilitates the removal of the gas that could diffuse through the membrane. Industrial nitrogen is used as the gas.

The cell with a deposit for solutions to control the relative humidity consists of a base and cover of high corrosion-resistant stainless steel (AISI 316L) and a cylindrical body of transparent material (methacrylate) with an internal border on which rests a ring-shaped glass deposit that contains the sulphuric acid solution (Figure 17).

The specimens have been obtained by uniaxial compaction of the clay directly in the oedometer ring. The clay was previously mixed with deionised water to reach 17 percent water content. The initial height of the specimen was 1.20 cm and its cross section 11.40 (for the dry density 1.79 g/cm^3) or 19.24 cm^2 (for the dry density 1.69 g/cm^3). The compaction pressure required to achieve these dry densities was between 32 and 38 MPa.

The tests were performed at a constant temperature of 20°C.

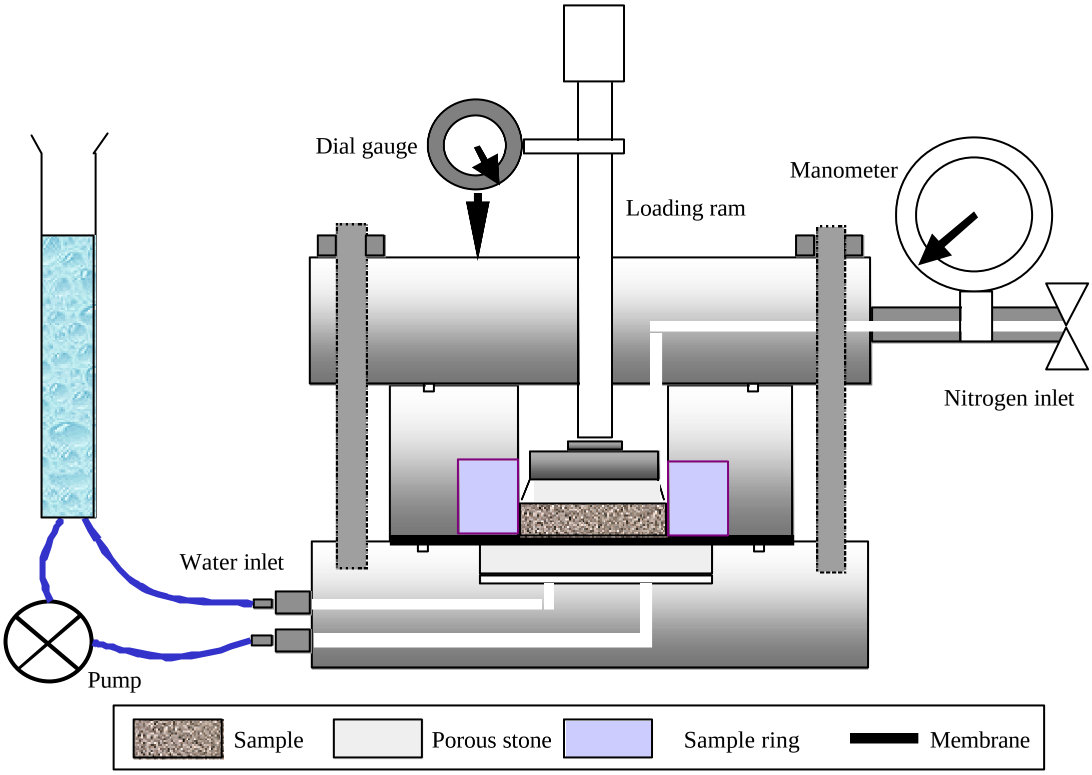

Figure 16: Schematic cross section of an oedometric membrane cell

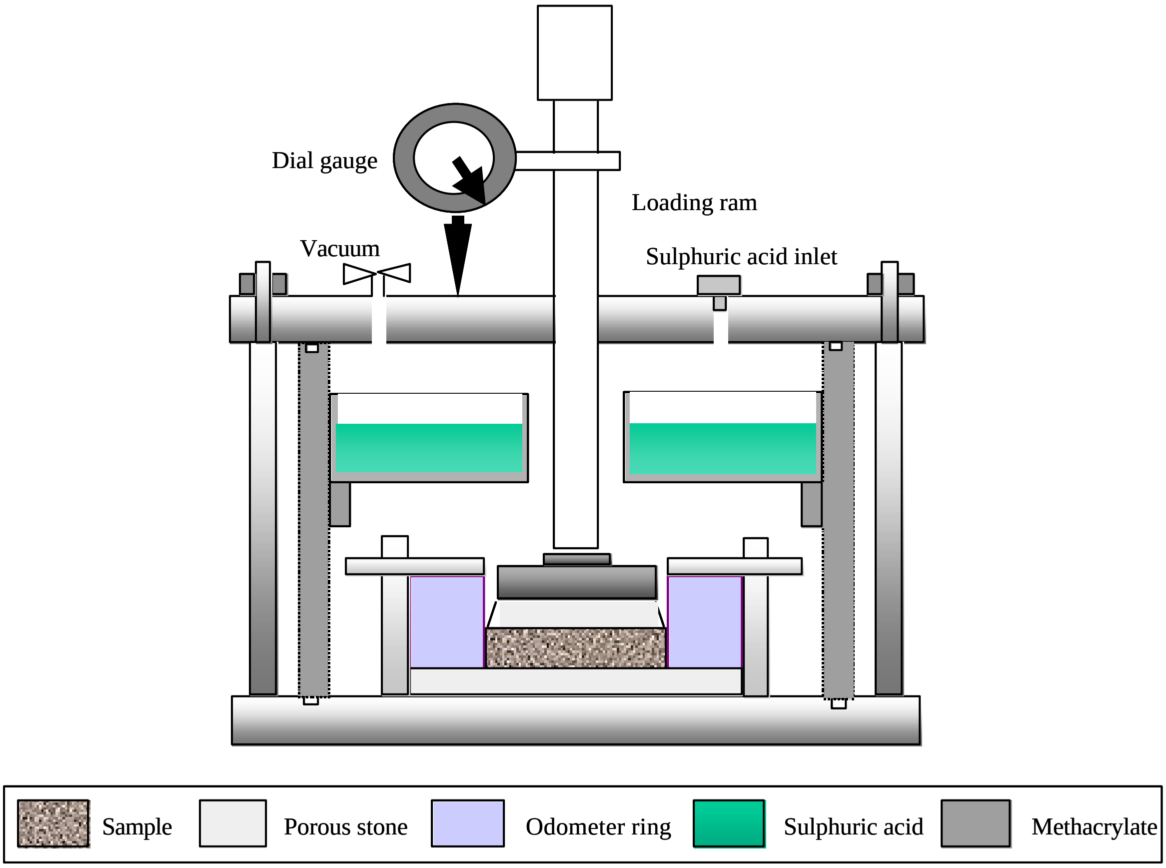

Figure 17: Schematic cross section of an oedometric cell with deposit for solutions

The samples have been subjected to hydration under a low vertical load and, once saturated, they have been loaded (Figure 18). The initial dry density and water content of the clay in these tests have been those of the blocks manufactured for the *in situ* test: nominal dry density 1.79 and 1.69 g/cm^3 and water content 17 percent. The two densities have been tested under both suction control methods. The maximum suction, 50 MPa, has been applied in the first step of the tests performed in sulphuric acid cells. It is the suction approximately corresponding to the initial water content of the specimens (see section 3.3) and, consequently, no major water content changes –and consequently, strain changes– were expected in this first step. The maximum vertical load applied has been 9 MPa for the higher density and 5 MPa for the lower one, which are the limits of the loading frames.

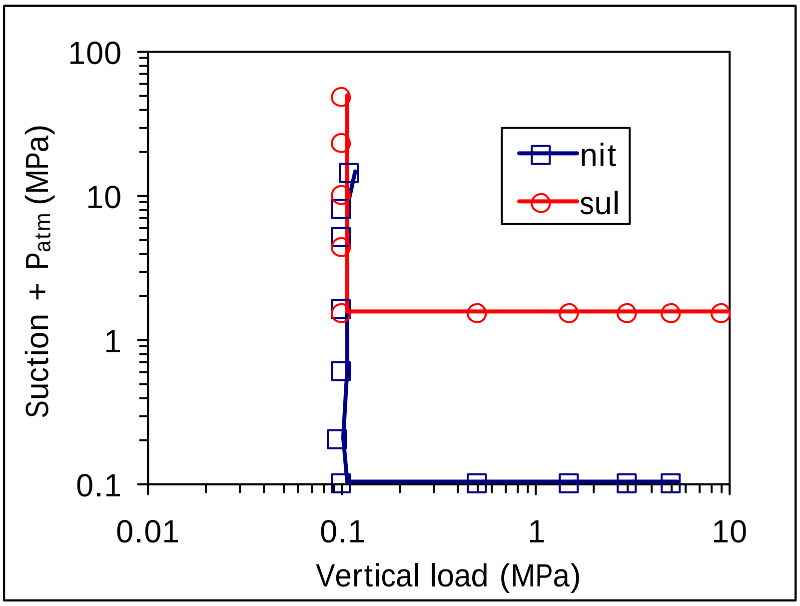

Figure 18: Stress path followed in the suction controlled oedometer test (nit: suction control by nitrogen pressure; sul: suction control by solutions)

3.5.2 Results

Four tests have been carried out, two with control of suction by nitrogen pressure and other two with control of suction by sulphuric acid solutions. The characteristics of the specimens at the beginning and end of the tests are shown in Table XI.

Table XI: Initial and final characteristics of the specimens tested

Test	**Suction control***	**Initial r$_{d}$ (g/cm^3)**	**Initial *w* (%)**	**Initial S_r (%)**	**Final r$_{d}$ (g/cm^3)**	**Final *w* (%)**	**Final S_r (%)**	**Duration (days)**
EDN4_10	Nit	1.69	17.4	73	1.52	40.0	131	633
EDN2_14	Nit	1.79	17.0	83	1.64	32.7	129	482
EDS4_9	Sul	1.69	17.0	72	1.50	34.3	110	1072
EDS2_13	Sul	1.79	16.2	80	1.64	31.1	122	1136

*Nit: suction control by nitrogen pressure, Sul: suction control by sulphuric acid solutions

The time required for stabilisation of each suction step is very long, much longer in the case of the tests in sulphuric acid cells, since the exchange of water in the vapour phase is slower. The stabilisation time becomes longer as the suction is lower, and thus, in the tests in sulphuric acid cells, the time to reach equilibrium for the lower suction (1 MPa) is more than one year (even longer for the test with higher initial dry density). As a result, the duration of the tests was longer than one year in nitrogen cells and of up to three years in the sulphuric acid cells (Table XI). The evolution of the strain as a function of time for the different steps of the tests is shown in Figure 19 to Figure 22. It can be observed that the swelling strain induced by the initial wetting (figures on the left) is not recovered during the subsequent loading (figures on the right) in any case. The behaviour of the bentonite in the final wetting step of the tests performed in sulphuric acid solution cells (Figure 21 and Figure 22) is particularly noticeable: the swelling takes place very slowly and seems to be endless, but the final vertical strain is not higher than that experienced by samples of the same initial dry density tested in nitrogen pressure cells under similar suction values.

Table XII to Table XV summarise the results of the oedometric test in terms of the characteristics of the samples at each step.

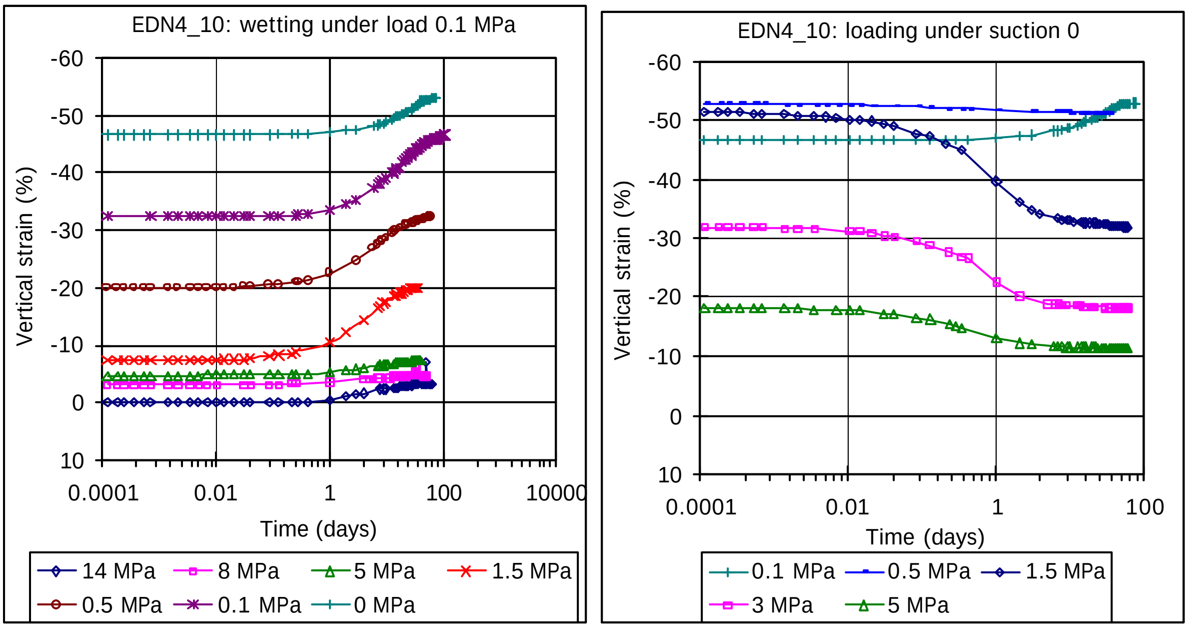

Figure 19: Evolution of strain in the different steps of test EDN4_10 (MX-80 compacted at ρ_d 1.69 g/cm^3)

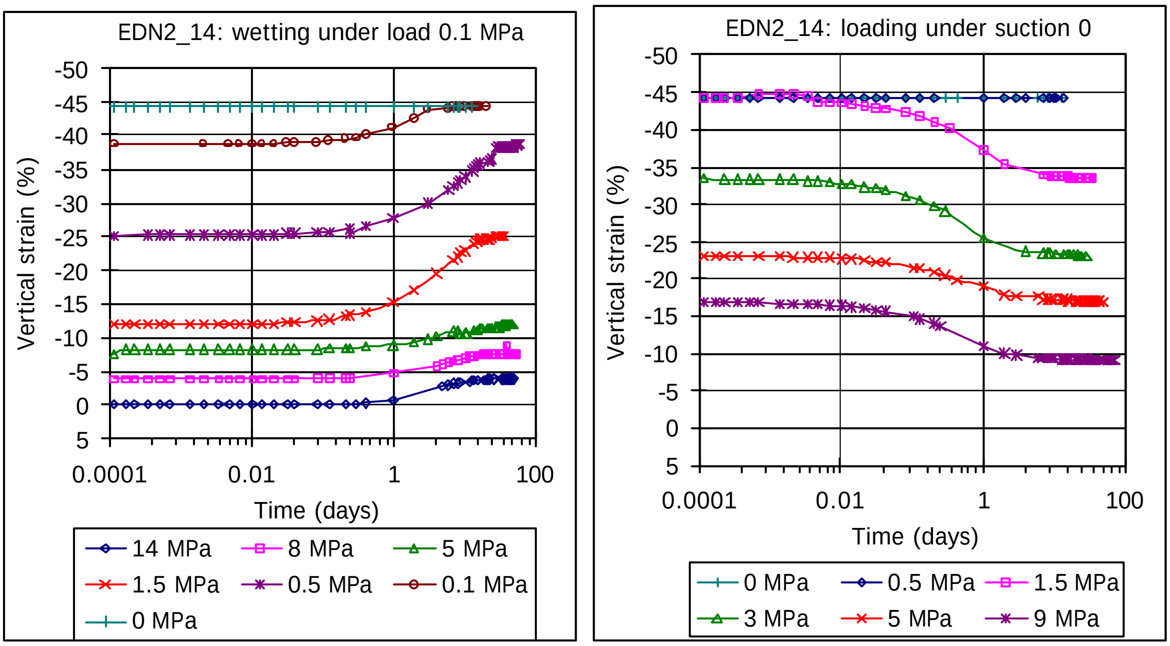

Figure 20: Evolution of strain in the different steps of test EDN2_14 (MX-80 compacted at ρ_d 1.79 g/cm^3)

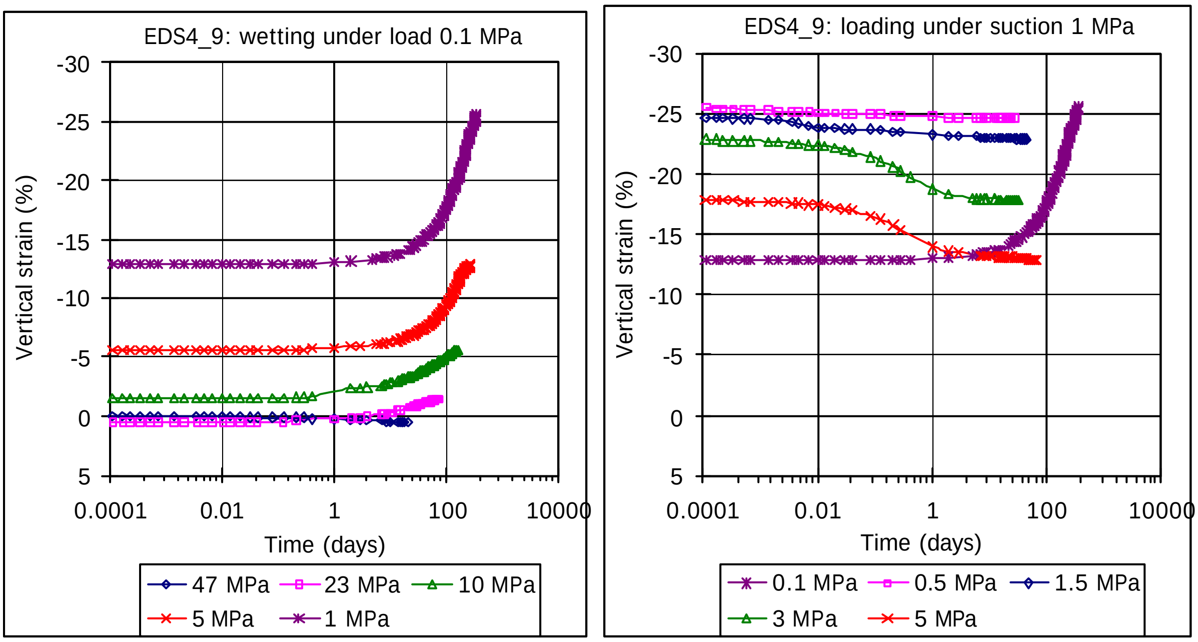

Figure 21: Evolution of strain in the different steps of test EDS4_9 (MX-80 compacted at ρ_d 1.69 g/cm^3)

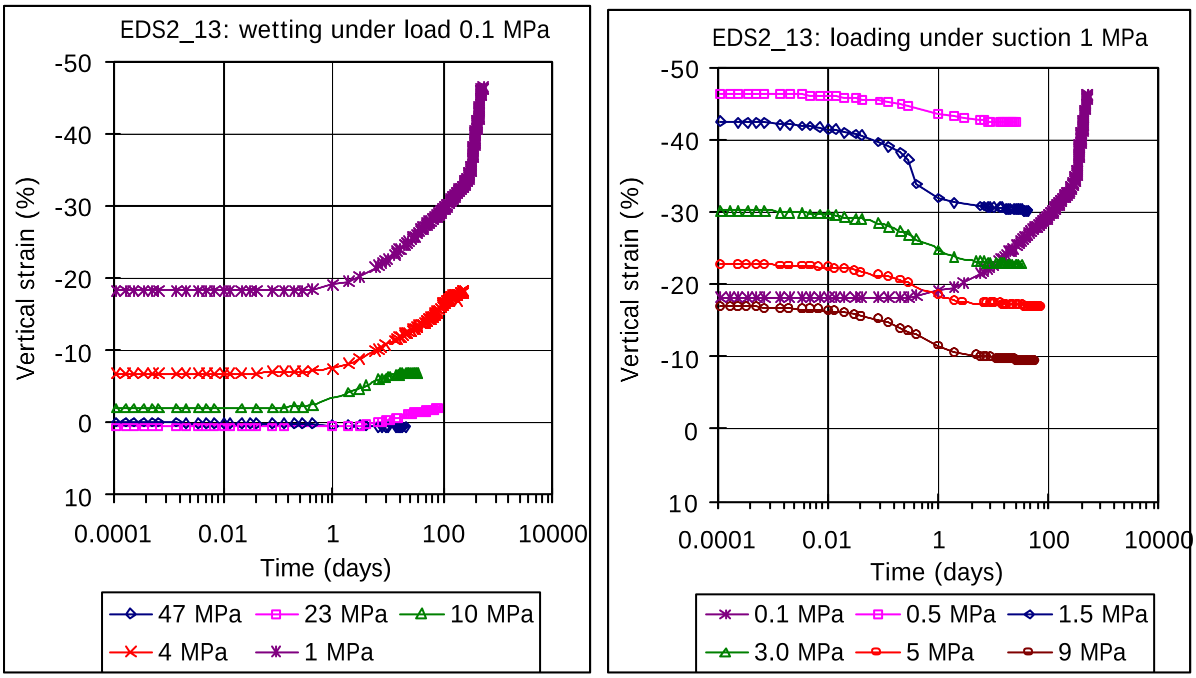

Figure 22: Evolution of strain in the different steps of test EDS2_13 (MX-80 compacted at ρ_d 1.79 g/cm^3)

Table XII: Results of the oedometric test EDN4_10

Step	**Initial r_d (g/cm^3)**	**Suction (MPa)**	**Vertical stress (MPa)**	**Final r_d (g/cm^3)**	**Final e**	**Duration (days)**
1	1.69	14.0	0.1	1.64	0.720	37
2	1.64	8.0	0.1	1.61	0.749	53
3	1.61	5.0	0.1	1.57	0.792	42
4	1.57	1.5	0.1	1.41	1.006	36
5	1.41	0.5	0.1	1.28	1.210	63
6	1.28	0.1	0.1	1.15	1.451	112
7	1.15	0.0	0.1	1.10	1.557	77
8	1.10	0.0	0.5	1.11	1.531	34
9	1.11	0.0	1.5	1.28	1.207	58
10	1.28	0.0	3.0	1.43	0.976	62
11	1.43	0.0	5.0	1.52	0.860	59

Table XIII: Results of the oedometric test EDN2_14

Step	**Initial r_d (g/cm^3)**	**Suction (MPa)**	**Vertical stress (MPa)**	**Final r_d (g/cm^3)**	**Final e**	**Duration (days)**
1	1.79	14.0	0.1	1.72	0.637	50
2	1.72	8.0	0.1	1.66	0.696	53
3	1.66	5.0	0.1	1.60	0.764	49
4	1.60	1.5	0.1	1.43	0.971	36
5	1.43	0.5	0.1	1.29	1.185	63
6	1.29	0.1	0.1	1.24	1.271	21
7	1.24	0.0	0.1	1.24	1.271	13
8	1.24	0.0	0.6	1.24	1.271	14
9	1.24	0.0	1.5	1.34	1.103	35
10	1.34	0.0	3.1	1.45	0.940	29
11	1.45	0.0	5.1	1.53	0.843	49
12	1.53	0.0	9.1	1.64	0.716	70

Table XIV: Results of the oedometric test EDS4_9

Step	**Initial ρ_d (g/cm^3)**	**Suction (MPa)**	**Vertical stress (MPa)**	**Final ρ_d (g/cm^3)**	**Final e**	**Duration (days)**
1	1.69	47.2	0.1	1.70	0.661	20
2	1.70	22.7	0.1	1.67	0.693	77
3	1.67	10.3	0.1	1.60	0.763	162
4	1.60	5.0	0.1	1.50	0.884	288
5	1.50	1.4	0.1	1.35	1.094	356
6	1.35	1.4	0.5	1.36	1.081	28
7	1.36	1.4	1.5	1.38	1.050	43
8	1.38	1.4	3.0	1.43	0.965	33
9	1.43	1.4	5.0	1.50	0.883	65

Table XV: Results of the oedometric test EDS2_13

Step	**Initial ρ_d (g/cm^3)**	**Suction (MPa)**	**Vertical stress (MPa)**	**Final ρ_d (g/cm^3)**	**Final e**	**Duration (days)**
1	1.79	47.2	0.1	1.80	0.564	20
2	1.80	22.7	0.1	1.76	0.604	77
3	1.76	9.8	0.1	1.68	0.682	36
4	1.68	4.3	0.1	1.52	0.860	238
5	1.52	1.4	0.1	1.22	1.302	532
6	1.22	1.4	0.5	1.26	1.241	28
7	1.26	1.4	1.5	1.38	1.049	43
8	1.38	1.4	3.0	1.46	0.931	33
9	1.46	1.4	5.0	1.53	0.839	72
10	1.53	1.4	9.0	1.64	0.721	57

The results obtained for the initial wetting of the four oedometric tests are plotted in Figure 23 in terms of final void ratios. A good agreement is found between the two methods of suction control, what, as in the case of the retention curves, would be an indication of the lack of repercussion of the osmotic suction on the behaviour of this bentonite. The initial difference in void ratio of the specimens is attenuated by the huge swelling developed for the lower suctions. A strange behaviour has been observed in the test performed in nitrogen oedometer for initial dry density 1.79 g/cm^3: the swelling trend changes for the lower suctions and seems to be hindered. However, after discarding mechanical obstructions, no other explanation has been found.

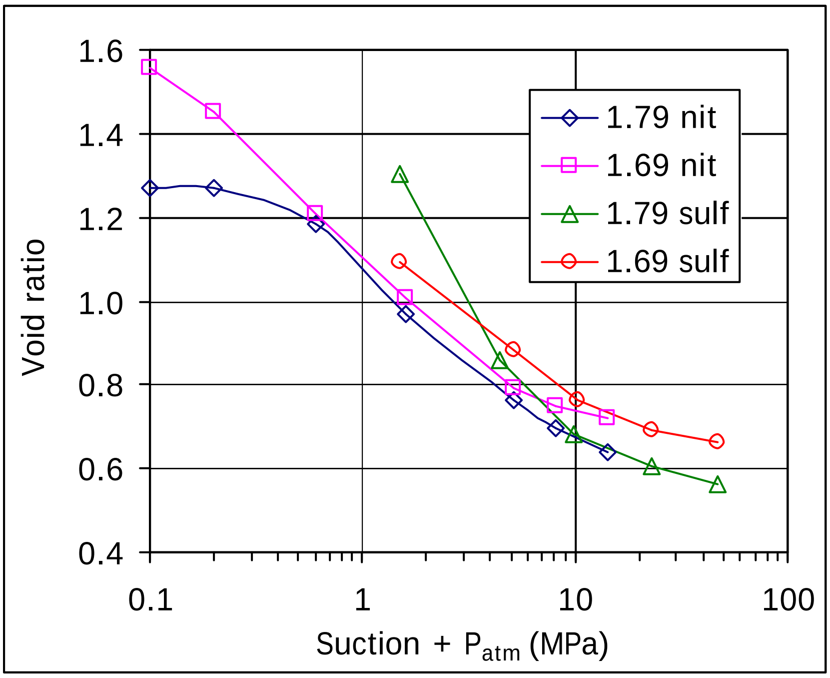

Figure 23: Void ratio evolution as a function of suction in the wetting path of the oedometric tests. MX-80 clay compacted to two densities (expressed in g/cm^3). Suction control by nitrogen pressure: nit, suction control by solutions: sulf

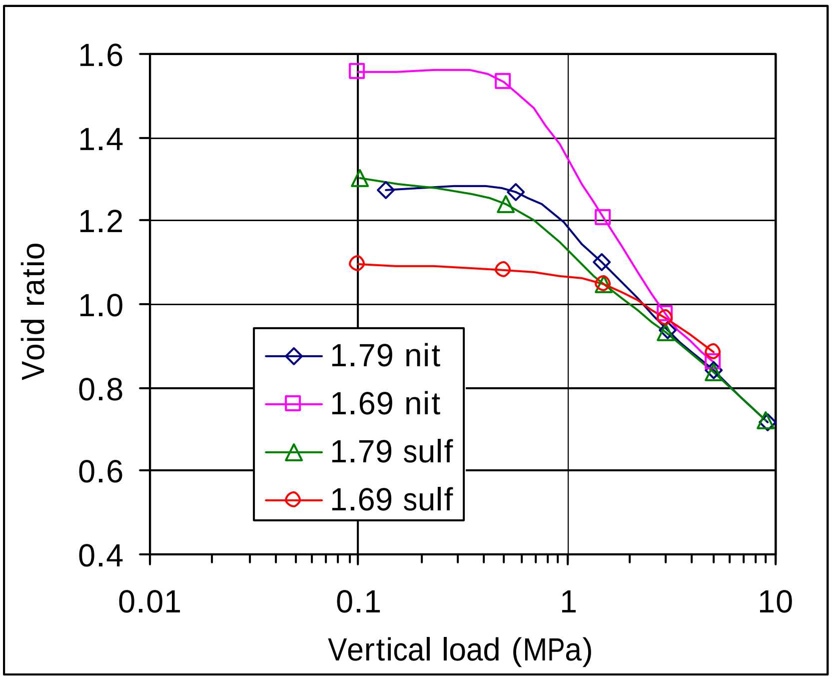

Figure 24: Oedometric curves of the loading paths performed after wetting

The oedometric curves of the loading paths after hydration (Figure 24) show that the apparent preconsolidation pressure is lower than 1 MPa, being lower for the test that reaches the highest void ratio during the previous wetting (test 1.69 nit). These values imply that the samples have experienced a decrease in the apparent preconsolidation pressure, since initially, it must have been similar to the pressure applied to compact the specimens, *i.e.* higher than 30 MPa. This decrease in apparent preconsolidation pressure is due to the microstructural changes induced during the saturation under a low vertical load, that has given place to a more open structure. The comparison of Figure 23 and Figure 24 makes again clear that the initial void ratio is not recovered at the end of the tests, what highlights the irreversibility of the deformations induced by hydration under low vertical loads.

On the other hand, the slope of the plastic part of the oedometric curves –which corresponds to the stiffness parameter for changes in stress, λ– is quite similar in all the tests.

4. COMPARISON OF THM BEHAVIOUR OF FEBEX AND MX-80 BENTONITES

The FEBEX bentonite was selected by ENRESA (Spain) as suitable material for the backfilling and sealing of HLW repositories, and it has been thoroughly characterised at CIEMAT. In fact, the Soil Mechanics Laboratory of CIEMAT has mainly worked with this bentonite for more than 10 years. Since the FEBEX and the MX-80 bentonites are different (particularly concerning their cationic exchange complex), and their THM behaviour has been extensively studied and modelled in several research projects, it has been considered of interest to compare their properties as determined by the same laboratory following the same methodologies. The results of this comparison are presented below.

The FEBEX bentonite comes from the Cortijo de Archidona deposit (Almería, Spain). A comprehensive characterisation of it exists (ENRESA 2000, Villar 2000, 2002, Fernández 2003, among others). The processing at the factory consisted in disaggregation and gently grinding, drying at 60°C and sieving by 5 mm. The smectite content of the FEBEX bentonite is higher than 90 percent (92±3 %). The smectitic phases of the FEBEX bentonite are actually made up of a montmorillonite-illite mixed layer, with 10-15 percent of illite layers. Besides, the bentonite contains variable quantities of quartz (2±1 %), plagioclase (2±1 %), K-felspar, calcite and opal-CT (cristobalite-trydimite, 2±1 %). The less than 2 µm fraction of this bentonite is 67±3 % of the total. The CEC varies from 96 to 102 meq/100g, and the major exchangeable cations are: Ca (35-42 meq/100g), Mg (31-32 meq/100g), Na (24-27 meq/100g) and K (2-3 meq/100g). The liquid limit of the bentonite is 102±4 %, the plastic limit 53±3 % and the specific weight is 2.70.

4.1 Saturated state

The swelling pressure (Figure 25) and the hydraulic conductivity (Figure 26) of the FEBEX and the MX-80 bentonites have been determined at CIEMAT following the methodologies described in sections 3.1.1 and 3.2.1. The results for the FEBEX bentonite have been taken from Villar (2000, 2002). In both cases the bentonite was compacted with its hygroscopic water content and saturated with deionised water. For the two bentonites the swelling pressure is exponentially related to dry density, being higher for the MX-80. On the other hand, the hydraulic conductivity of the MX-80 is slightly higher (up to half an order of magnitude for the same dry density) than that of the FEBEX bentonite.

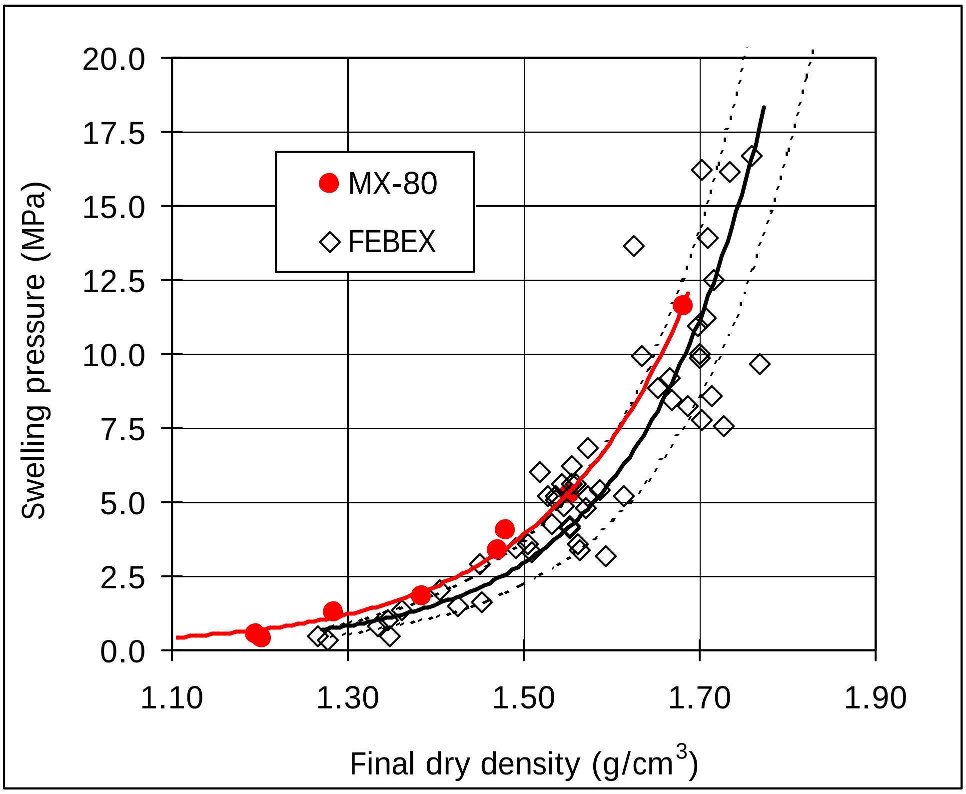

Figure 25: Swelling pressure of MX-80 and FEBEX bentonites compacted with their hygroscopic water contents and saturated with deionised water

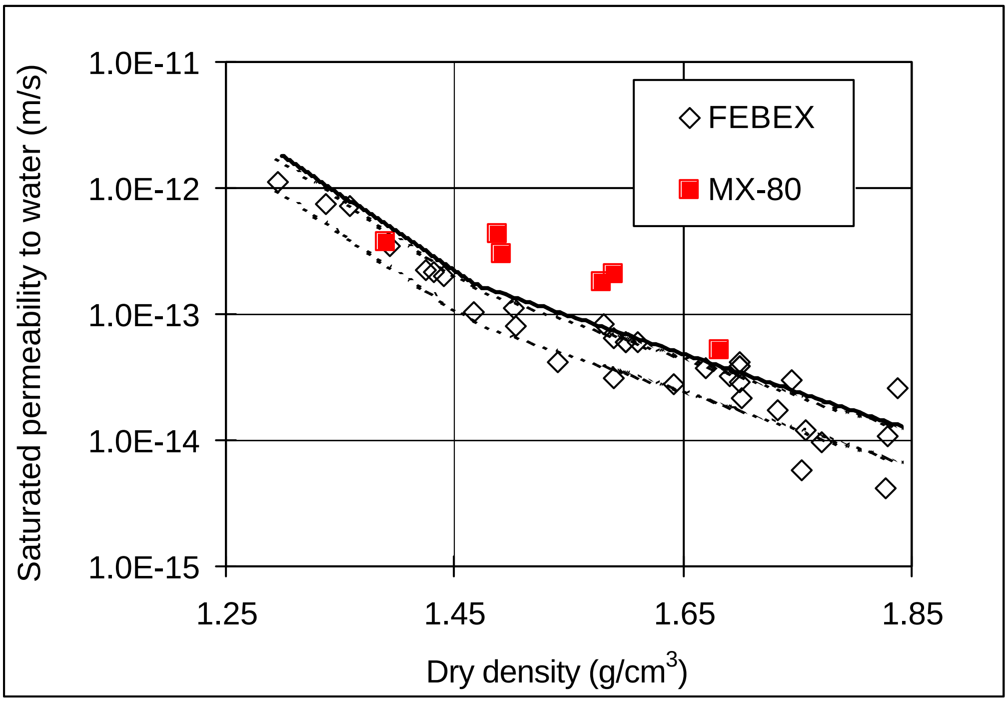

Figure 26: Permeability to deionised water of FEBEX and MX-80 bentonites compacted at different dry densities

4.2 Unsaturated state

4.2.1 Retention curves

The dependence of suction on water content has been determined by means of the sensor/block method –as described in section 3.3.1– for the two bentonites. The results corresponding to the bentonite mixed with deionised water are plotted in Figure 27. It can be observed that the retention capacity of the FEBEX bentonite is higher, *i.e.* for a given suction and dry density, the water content of the FEBEX bentonite is higher. However, the difference between both bentonites becomes smaller towards the lower suctions and, although there are not enough data, it seems that below 10 MPa the two bentonites behave similarly.

This comparison can be also made for the curves obtained at 60°C with the cells method. The results for the FEBEX bentonite have been taken from Lloret *et al.* (in press), and are plotted in Figure 28 along with the results for MX-80 reported in Table IX. From the Figure it follows, on the one hand, that the difference in the retention capacity of the two bentonites observed at 20°C is less important at high temperature, and seems to disappear for suctions lower than 50 MPa. On the other, that the hysteretic behaviour is more important for FEBEX than for MX-80.

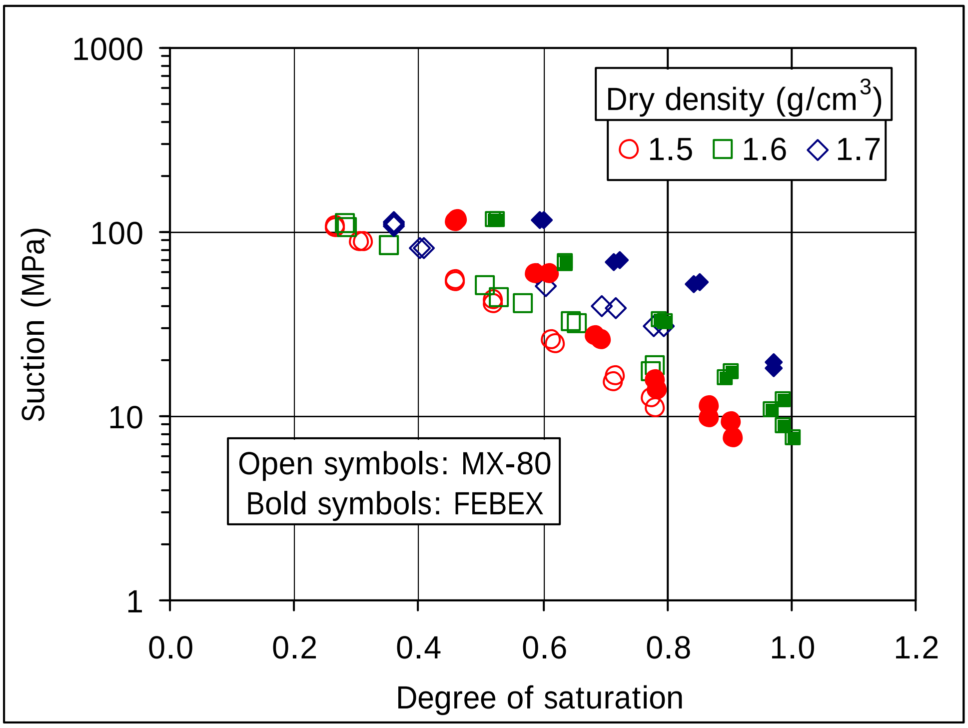

Figure 27: Retention curves obtained at 20°C with the sensor/block method for two bentonites compacted at different dry densities

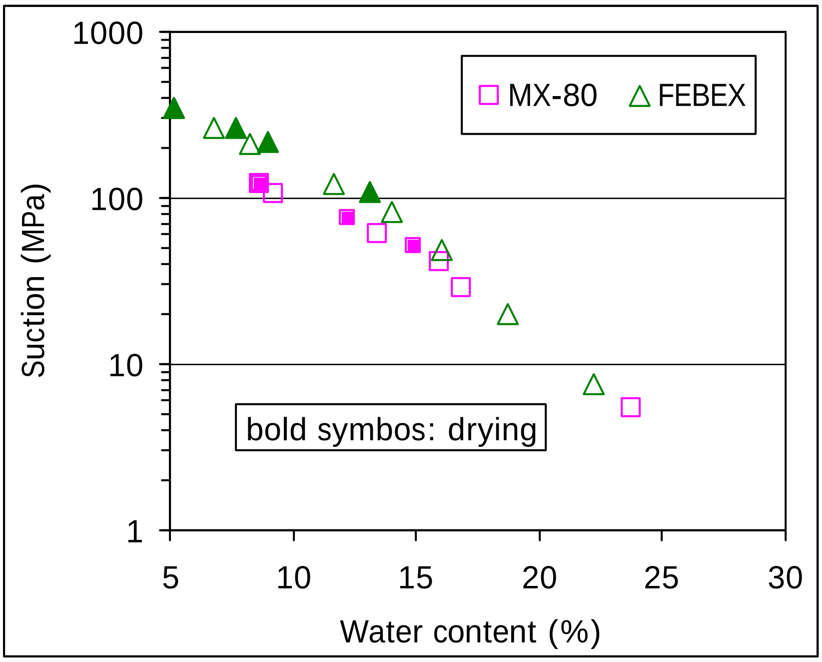

Figure 28: Retention curves obtained at 60°C with the cells method in drying/wetting paths for two bentonites compacted at nominal dry density 1.60 g/cm^3

4.2.2 Oedometric behaviour

One of the oedometric tests performed with MX-80 and reported herein, the EDS4_9, has been compared with tests performed with the FEBEX bentonite that followed similar stress paths, *i.e.* wetting under a low vertical load (0.1 MPa) and loading under a suction of 1 MPa. In these tests, which are reported in Villar (2002), the bentonite was initially compacted to nominal dry density 1.70 g/cm^3 with its hygroscopic water content (14 percent). The initial conditions of the test performed with MX-80 were: initial dry density 1.69 g/cm^3 and initial water content 17 percent.

All the tests performed with the FEBEX bentonite started with the sample subjected to a suction higher than that used with MX-80, which was 50 MPa. Test EDS2-9 started with a suction of 120 MPa and was finished after reaching a suction of 4 MPa. Tests EDS4_8 and EDS5_5 started by first drying the bentonite under a low vertical load and then wetting it. It has been observed that this initial drying does not have a major repercussion on the subsequent behaviour of the bentonite (Villar 2002). The behaviour of the two bentonites on wetting under a low vertical load is shown in Figure 29 (left). Although the final swelling is similar for both, it seems that the MX-80 develops most of the swelling when the low suctions are reached. This is in accordance with the results obtained in the retention curves. The behaviour upon loading can be seen in Figure 29 (right). Although the void ratio at the beginning of loading is almost the same for the two bentonites, the compressibility of the FEBEX bentonite is higher. Nevertheless, the deformations induced during the initial wetting are not completely recovered upon loading for any of these bentonites.

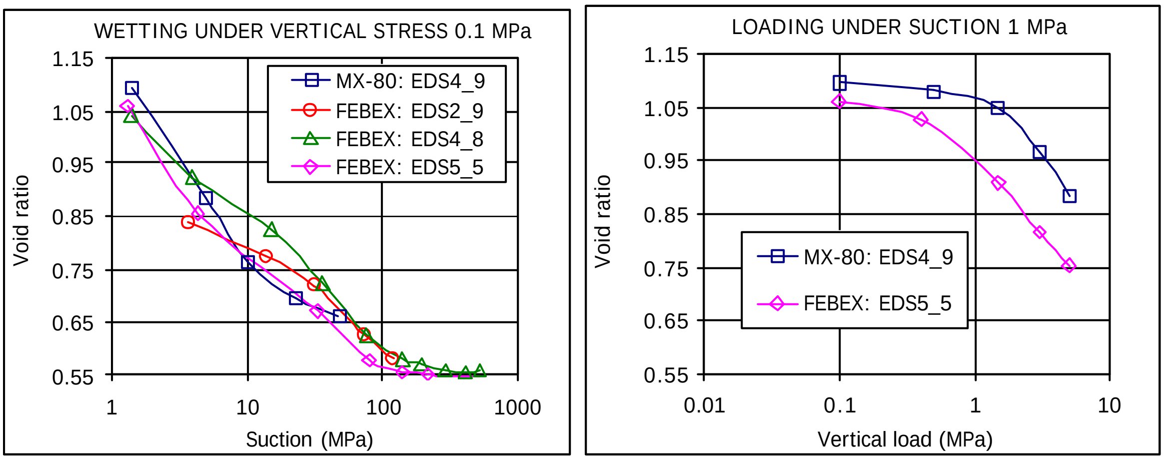

Figure 29: Evolution of void ratio in suction controlled oedometric tests performed with MX-80 and FEBEX bentonites compacted at initial ρ_d 1.7 g/cm^3

5. SUMMARY AND CONCLUSIONS

The results of the thermo-hydro-mechanical (THM) characterisation of the MX-80 bentonite performed by CIEMAT from 2001 to 2004 in the context of the Prototype Repository Project have been presented.

The swelling pressure of the bentonite compacted to different dry densities and saturated with deionised water has been determined. An exponential relation between swelling pressure and dry density has been found.

The hydraulic conductivity of the bentonite compacted to different dry densities has been determined using deionised and saline water as permeants. The hydraulic conductivity is 135 percent higher when water of 0.5 percent salinity is used as permeant.

To study the influence of salinity on the retention capacity of the compacted bentonite, a new methodology has been designed and its correct performance checked. The results clearly show the dependence of suction on degree of saturation, being the suction of a block of a given degree of saturation higher the higher the dry density of the block. It has not been possible to distinguish the influence of the salinity of the interstitial water on the value of suction, what indicates that it is not relevant and that the matric suction must predominate over the osmotic at least for salinities of up to 0.5 percent.

The water retention curves of the bentonite compacted at various dry densities have been determined at temperatures of 20 and 60°C following different paths. The effect of temperature on the retention capacity is very small. The hysteresis effects are neither important.

Four suction controlled oedometer tests have been performed at 20°C. The bentonite has been initially wetted under a low vertical load and then loaded. The swelling strain induced by the initial wetting is not recovered during the subsequent loading. Besides, the apparent preconsolidation pressure after the initial wetting is lower than 1 MPa, what means that the samples have experienced a decrease in the apparent preconsolidation pressure from the initial value. This decrease in apparent preconsolidation pressure is due to the microstructural changes induced during the saturation under a low vertical load, that has given place to a more open structure.

Finally, the behaviour of the MX-80 bentonite has been compared to that of the Spanish FEBEX bentonite. The swelling pressure of the MX-80 is higher than that of the FEBEX, whereas, the hydraulic conductivity of the MX-80 is slightly higher (up to half an order of magnitude for the same dry density) than that of the FEBEX bentonite. On the other hand, the retention capacity of the FEBEX bentonite is higher, but the difference between both bentonites becomes smaller towards the lower suctions. The same is observed at 60°C, although the difference between both bentonites is even less important. Besides, the hysteretic behaviour is more important for FEBEX than for MX-80. With respect to the behaviour of both bentonites under suction controlled oedometric conditions, it has been seen that the MX-80 develops most of the swelling when the low suctions are reached and that the compressibility of the FEBEX bentonite is higher.

6. ACKNOWLEDGEMENTS

The research agreement CIEMAT/ENRESA 00/271, carried out under the CIEMAT/ENRESA General Agreement, has financed this research. Dr. P.L. Martín (CIEMAT) collaborated in the design of the methodology to determine the retention curves. The collaboration of Dr. A. Ledesma from UPC (Technical University of Catalonia, Spain) in the design of the oedometric tests is gratefully acknowledged. The laboratory work has been performed at the Soil Mechanics Laboratory of CIEMAT (Madrid, Spain) by R. Campos and J. Aroz.

7. REFERENCES

ENRESA 2000. FEBEX Project. Full-scale engineered barriers experiment for a deep geological repository for high level radioactive waste in crystalline host rock. Final Report. Publicación Técnica ENRESA 1/2000. 354 pp. Madrid.

Fernández, A.M. 2003. Caracterización y modelización del agua intersticial en materiales arcillosos. Estudio de la bentonita de Cortijo de Archidona. Ph. D. Thesis. Universidad Autónoma de Madrid, 505 pp. (In Spanish).

Gmitro & Vermeulen 1964. An I. Ch. E. J. 10(5): 740.

Karnland, O.; Pusch, R. & Sandén, T. 1992. The importance of electrolyte on the physical properties of MX-80 bentonite. SKB Report AR 92-35. Stockholm. (In Swedish).

Lide, D.R. 1995. CRC Handbook of Chemistry and Physics. 75th ed. CRC Press.

Lloret, A.; Villar, M.V. & Romero, E. (in press): Final report on thermo-hydro-mechanical laboratory tests. Deliverable D17/3. Publicación Técnica ENRESA. Madrid

Marcial, D. 2003. Comportement hydromécanique et microstructural des matériaux de barrière ouvragée. Ph. D. Thesis. École Nationale des Ponts et Chausées, Paris. 316 pp. (In French).

Müller-Vonmoss, M. & Kahr, G. 1983. Mineralogische Untersuchungen von Wyoming Bentonite MX-80 und Montigel. NTB 83-13. NAGRA, Wettingen. (In German).

van Genuchten, M. Th., 1980. A closed-form equation for predicting the hydraulic conductivity of unsaturated soils. Soil Sci. Soc. Am. J. 44: 892-898.

van Genucthen, M. Th., Leij, F.J. & Yates, S.R., 1991. The RETC code for quantifying the hydraulic functions of unsaturated soils. U.S. Salinity Laboratory IAG-DW12933934. U.S. Environmental Protection Agency EPA/600/2-91/065. Riverside.

Villar, M.V., 2000. Caracterización termo-hidro-mecánica de una bentonita de Cabo de Gata. Ph. D. Thesis, Universidad Complutense de Madrid, Madrid. 396 pp. (In Spanish).

Villar, M.V. 2002. Thermo-hydro-mechanical characterisation of a bentonite from Cabo de Gata. A study applied to the use of bentonite as sealing material in high level radioactive waste repositories. Publicación Técnica ENRESA 01/2002. 258 pp. Madrid.

Villar, M.V. & Lloret, A. 2004. Influence of temperature on the hydro-mechanical behaviour of a compacted bentonite. Applied Clay Science 26: 337-350.